The Thesis Committee for Keren Arunothayam Thomas Muthiah
Certifies that this is the approved version of the following thesis:

Synthesis and Stabilities of Mononuclear Iron (II) Dicarbonyls derived from Neutral NNS Ligands: Structural Models of the Apo-active Site of Mono-Iron (Hmd) Hydrogenase

APPROVED BY
SUPERVISING COMMITTEE:

Supervisor:

Michael J. Rose

Bradley J. Holliday

Synthesis and Stabilities of Mononuclear Iron (II) Dicarbonyls derived from Neutral NNS Ligands: Structural Models of the Apo-active Site of Mono-Iron (Hmd) Hydrogenase

by

Keren Arunothayam Thomas Muthiah, M.S.

Thesis

Presented to the Faculty of the Graduate School of

The University of Texas at Austin

in Partial Fulfillment

of the Requirements

for the Degree of

Master of Arts

The University of Texas at Austin

August 2014

Dedication

I dedicate this thesis to my Lokhesh and my parents for their love and support.

Acknowledgements

I praise and thank God for providing me this opportunity. I would like to extend my thanks to everyone who guided and supported me through these two years of my life at UT Austin.

Dr. Michael Rose, my advisor, for his guidance and his mentorship. I would also like to thank all my professors. I thank and acknowledge the contribution of the past and present members of the Rose Group in my project. I thank Dr.Vincent Lynch for solving tricky crystal structures and Steve Sorey for the NMR measurements.

I must thank my friends from the neighboring labs who let me borrow chemicals and instrument time when I most needed them.

Abstract

Synthesis and Stabilities of Mononuclear Iron (II) Dicarbonyls derived from Neutral NNS Ligands: Structural Models of the Apo-active Site of Mono-Iron (Hmd) Hydrogenase

Keren Arunothayam Thomas Muthiah, M.A.

The University of Texas at Austin, 2014

Supervisor: Michael J. Rose

Herein is described the syntheses and characterization of iron dicarbonyl complexes derived from tridentate *ortho*-substituted Schiff base pyridine/thioether ligands ($_R$NNS) and $[Fe(CO)_4(Br)_2]$. Two general synthetic routes are reported for the isolation of such iron carbonyls. First, metalation of $_R$NNS ligands within Et_2O at room temperature affords the complex species of type $[(_RNNS)Fe(CO)_2Br][Fe(CO)_3(Br)_3]$. Alternatively, metalations of $_R$NNS (R = CH_3, OCH_3) at low temperature (−78 °C) in CH_2Cl_2/MeCN mixtures with $[Fe(CO)_4(Br)_2]$ afford complexes of formula $[(_RNNS)Fe(CO)_2Br]Br$. Reactions under similar conditions with more sterically demanding ligands [R = quinoline (Q), chlorophenyl (ClPh)] afford a complex salt of the form $[(_RNNS)Fe(CO)_2Br][Fe(CO)_3(Br)_3]$. Complexes have been characterized using X-ray crystallography, IR spectroscopy and low temperature ^{1}H NMR spectroscopy. Photostability of the complexes has been studied using UV-vis and solution IR spectroscopies. Relevance to the apo-active site of mono-iron hydrogenase is discussed.

Table of Contents

I.A. Introduction to the Hydrogenase Enzyme

Introduction to The Third Hydrogenase

Hydrogenases are enzymes found in archaea and bacteria that catalyze either the production or utilization of dihydrogen (H_2). These enzymes have captured the interest of the scientific and industrial circle as they use dihydrogen as the reducing agent. The two most commonly known hydrogenases are the [FeFe]-hydrogenase, which contains iron-sulfur clusters and [NiFe]-hydrogenase, which contains nickel and iron-sulfur clusters. The [NiFe]-hydrogenase also includes hydrogenases that contain selenium, [NiFeSe]-hydrogenase (Figure I.1).

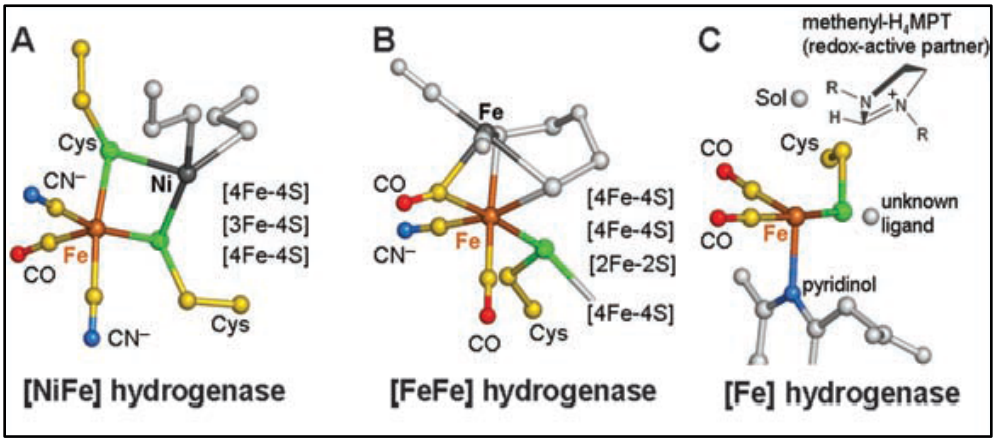

Figure I.1 The active sites of the Hydrogenases (A) [NiFe]-hydrogensase from *Desulfovibrio gigas*. (B) [FeFe]-hydrogenase from *Clostridium pasteurianum* and *Desulfovibrio desulfuricans*. (C) [Fe]-hydrogenase from *Methanocaldococcus Jannaschii* (Figure credits to Shima *et al*.).[1]

In the 1980s, a third type of hydrogenase was found to be the mononuclear iron hydrogenase (also known as H_2-forming methylenetetrahydromethanopterin dehydrogenase (Hmd)). This hydrogenase does not contain any nickel, or iron-sulfur clusters and therefore is also known as the 'iron-sulfur-cluster free' hydrogenase. This

enzyme is sensitive to light (prone to bleaching) and dioxygen and therefore is grown under red light. Additionally, Hmd is only constitutively expressed under nickel-limiting conditions, which prevents the production of the otherwise preferable [NiFe] hydrogenase. Hmd catalyzes the reversible reduction of methenyl-tetrahydromethanopterin (methenyl-H_4 MPT^+) with H_2 to methylene-H_4 MPT and H^+ (Scheme I.1). This reaction is an intermediate step in the production of methane from carbon dioxide.[1]

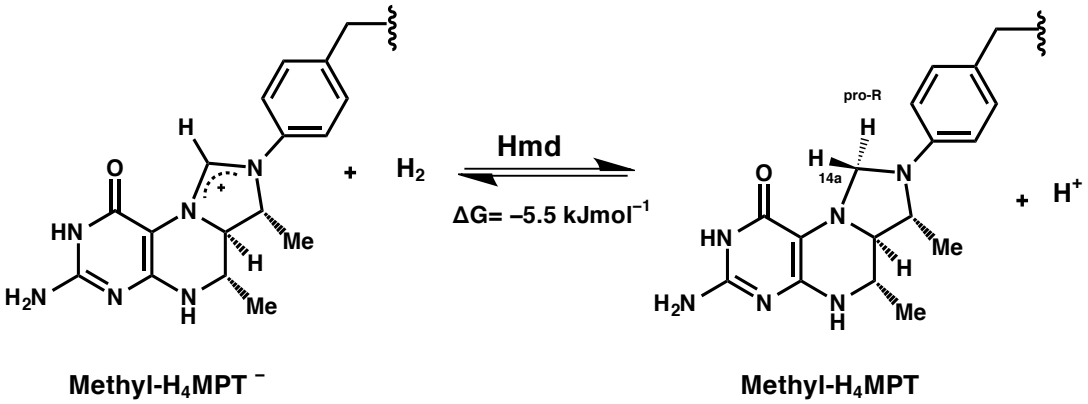

Scheme I.1 Reaction catalyzed by Hmd, i.e. [Fe]-hydrogenase.

Crystal structure of the active site of [Fe]-Hydrogenase

For many years, the structure of the active site of Hmd was a matter of intense debate due to difficulty in obtaining pure enzyme and crystallization of the protein. NMR spectroscopy and mass spectrometry were initially used to characterize Hmd, as well as its active site cofactor. For several years it was believed that this hydrogenase did not contain any metal site and that it was a purely organic active site. Subsequently it was

discovered that the activity of the enzyme was dependent on the presence of an iron cofactor and the crystal structure of the enzyme was reported. Mössbauer spectroscopy was used to identify the oxidation state of metal center. It was concluded that the metal was either low spin Fe(0) or Fe(II)[2] and that the iron center in the active site was not redox-active.

In 2008, Shima *et al*. reported the first crystal structure of the active site of Hmd with the Fe (II) center. The coordination of the central metal is as follows: iron is

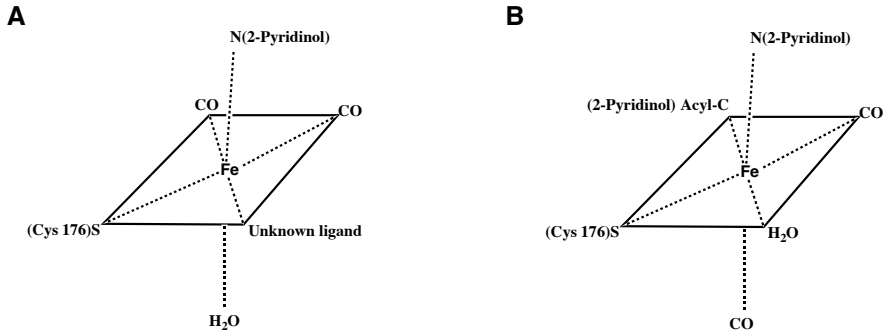

Figure I.2 Originally proposed model (A) and revised model (B) of the active site [Fe]-Hydrogenase.

coordinated to Cys[176] sulfur, two CO molecules, and an unknown ligand in the equatorial plane of the Fe(II) center octahedron. The nitrogen from 2-pyrinidol/2-pyridone is in the pyramid. The sixth position is occupied by a solvent molecule (H_2O), which was suggested to be the binding site of substrate H_2 (Figure I.2.A).[3]

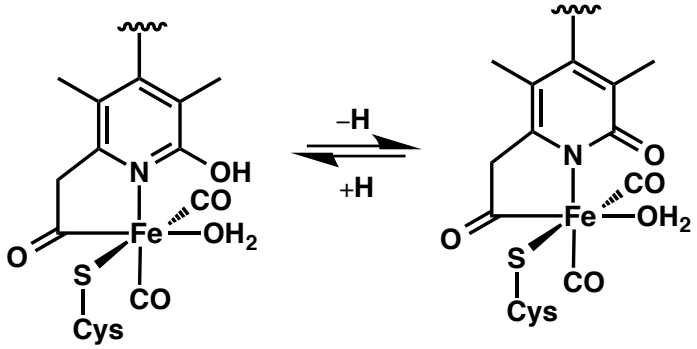

Figure I.3 The active site on [Fe]-Hydrogenase.

The proposed structure **A** was revised and the new structure **B** is widely accepted. In this, the iron is octahedrally coordinated to the sulfur of Cys[176], two CO molecules, an acyl unit from the 2-pyridinol 6-formylmethyl group and the nitrogen of the same moiety, the solvent/substrate is present *trans* to the acyl unit (Figure I.3). Fe(II) is in the low spin state and the acyl unit carries a negative charge, while possibly also acting as a strong π-acceptor.

Biogenesis of the Active Site of Hmd

For many decades it was believed that the only known naturally occurring bioorganometallic compound was Vitamin B_{12}. It was the only known compound to have a stable metal-carbon bond other than a carbonyl ligand. Now the only other known biological complex to have this unique feature is the [Fe]-Hydrogenase, and this distinct acyl unit is like no other bond yet found in biology.

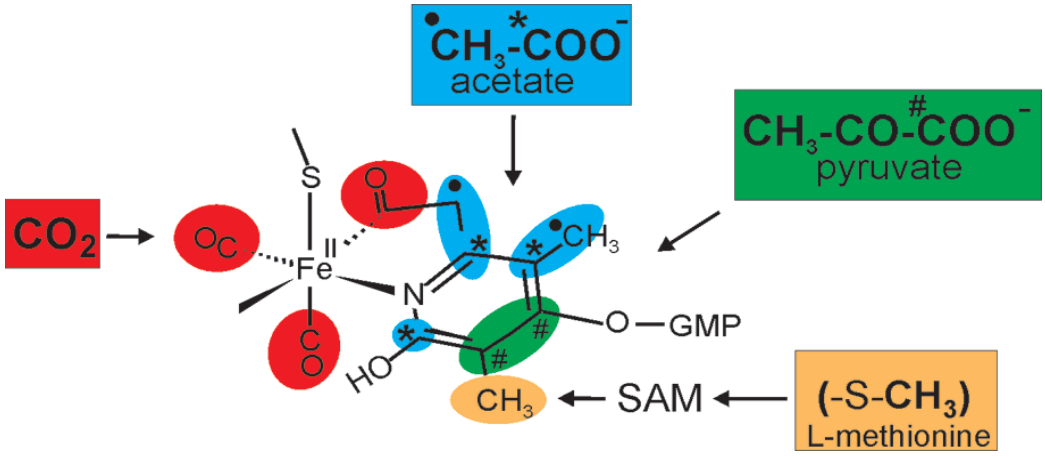

Figure I.4 The predicted biosynthesis of FeGP. (Picture credits to Shima *et al.*)[4]

Shima *et al*. have investigated the biogenesis of the active site of Hmd using stable-isotope labeling experiments (Figure I.4).[4] Labeling studies show that the methyl group in the *para*-position relative to the alcohol in the pyridinol ring has been derived from the methyl group of the methionine. The biogenesis of the two CO ligands and acyl unit were traced using labeling experiments employing acetates and pyruvates containing appropriate substitution with ^{13}C. These studies revealed that the ligands were not derived from these precursors. Later $^{13}CO_2$ was used to in similar studies using different mass spectrometry techniques. These studies indicated that CO_2 was the precursor of these three ligands in Hmd. However, the exact mechanism of the formation of the unique acyl bond still remains unclear. The authors proposed a mechanism based on the formation of the acetyl-nickel bond from the acetyl-CoA synthase/decarbonylase of acetogens and methanogens.

To further understand the structural implications and the role of each component of the active site, synthetic modeling becomes an attractive approach. Synthetic modeling of the active site gives the flexibility to incorporate a few or all of the features of the active site and then study their individual contributions to the stability or the property of the active site.

1.4. References

(1) Shima, S.; Pilak, O.; Vogt, S.; Schick, M.; Stagni, M. S.; Meyer-Klaucke, W.; Warkentin, E.; Thauer, R. K.; Ermler. U. *Science* **2008,** *321*, 25.

(2) Wang, X.; Li, Z.; Zeng, X.; Luo, Q.; Evans, D. J.; Pickett, C. J.; Liu, X. *Chem. Commun*. **2008**, 3555.

(3) Hiromoto, T.; Ataka, K.; Pilak, O.; Vogt, S.; Stagni, M. S.; Meyer-Klaucke, W.; Warkentin, E.; Thauer, R. K.; Shima, S.; Ermler. U. *FEBS Lett*. **2009**, *583*, 585.

(4) Schick, M.; Xie, X.; Ataka, K.; Kahnt, J.; Linne, U.; Shima, S. *J. Am. Chem. Soc*. **2012**, *134*, 3271.

I.B. Literature Survey: Synthetic Models of Mono-Iron Hydrogenase present in the Literature

Ferracyclic carbamoyl complexes related to the active site of [Fe]-Hydrogenase[1]

The active site of the [Fe]-hydrogenase or H_2-forming methylenetetrahydromethanopterin dehydrogenase (Hmd) contains only one iron(II) in the active site. There is much interest in the unique array of ligands, which bind to the metal center to form the active site. This consists of two *cis*-carbonyl groups, a chelating pyridine–acyl ligand, a sulfur of *Cys*176 and a solvent molecule (presumably H_2O). Pickett *et al*. have reported ferracyclic complexes with carbamoyl group as a substitute for acyl unit. The general scheme for the preparation for the carbamoyl unit is given in Scheme I.2.

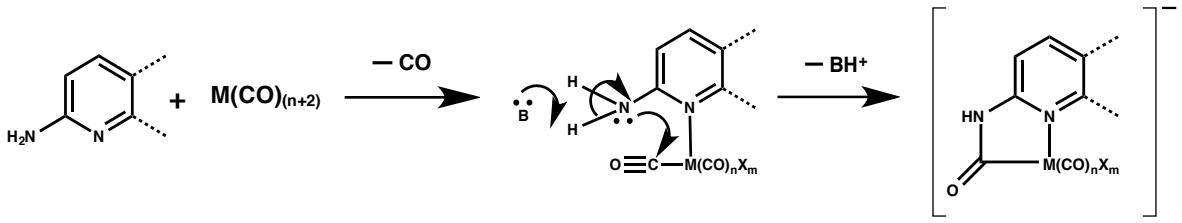

Scheme I.2 Generalized mechanism for metallocyclic carbamoyl formation.

The initial reaction with of 2-aminopyridine with $[Fe(CO)_4Br_2]$ forms the carbomyl unit. This complex contains a labile solvent molecule, which can be replaced by more strongly coordinating ligands such as PR_3 (R = Me, Ph). The replication of the active-site with a replacable solvent coordination site was sucessfully charaterized by X-ray crystallography. Attempts to introduce a hydroxyl group, using the ligands **1a, 1a'** and **1b**, at the 6-position of the pyridine were unsucessful (Figure I.5).

1a R=H
1b R=Si(i-Pr)$_3$

1a'

Figure I.5 Oxygen-functionalized aminopyridines.

On the contrary, reaction with 2,6-diaminopyridine, which has an additional nitrogen pendant base at the 6-position, undergoes reaction similar to 2-aminopyridine.

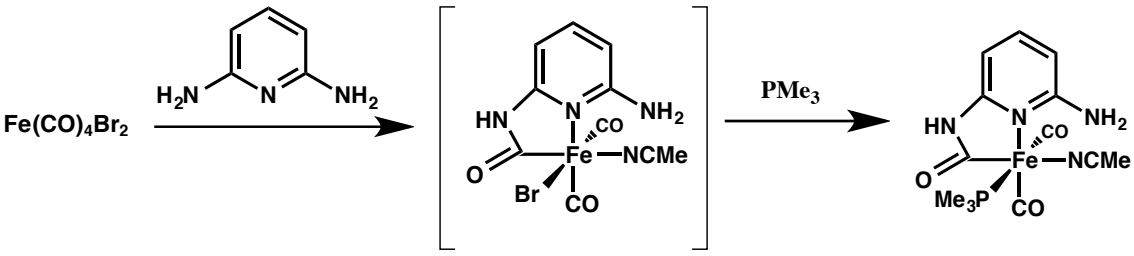

2 **3**

Scheme I.3 Synthesis of complex **3**.

The structure of compound **3** was characterized by X-ray crystallography. This compound is structurally similar to the active site as it contains an alternative pendant base in the place of hydroxyl group at the 6-position (Scheme I.3).

Biomimetic Models for the Active Site of [Fe]-Hydrogenase Featuring an Acylmethyl(hydroxymethyl)pyridine Ligand[2]

Li-Cheng Song *et al*. have synthesized novel model complexes of [Fe]-Hydrogenase containing acylmethyl (hydroxymethyl) pyridine ligand by the following scheme (Scheme I.4).

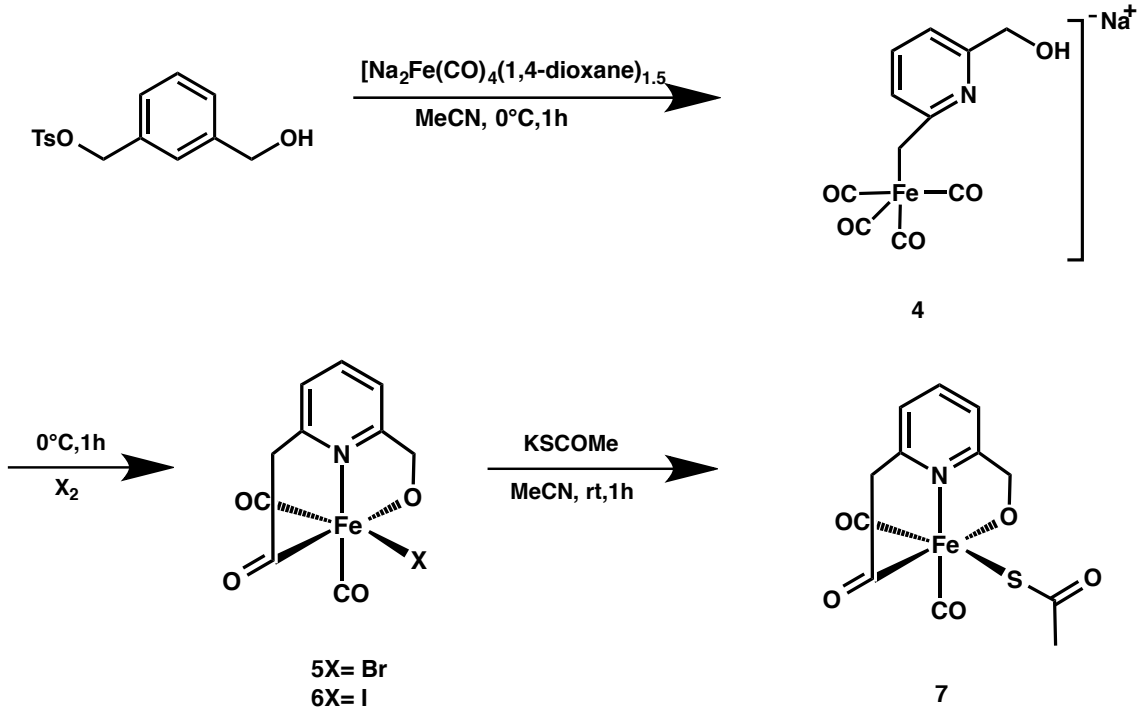

Scheme I.4 Synthesis of Model Complexes **5**− **7** via Intermediate Complex **4**.

The synthetic route proposed uses the formally Fe(−2) salt of $[Na_2Fe(CO)_4$ (1,4-dioxane)$_{1.5}]$, which undergoes oxidative addition during the nucleophilic substitution with 2-(4-$MeC_6H_4SO_3CH_2$)-6-$HOCH_2C_5H_3N$ in MeCN to give the Fe(0) complex salt [Na(2-CH_2-6-$HOCH_2C_5H_3N$)$Fe(CO)_4$] **(4)**. In the presence of Br_2 or I_2, *in situ* CO migratory

insertion followed by coordination of its hydroxyl group and oxidation of the metal site result in the formation of the model complexes [(2-$COCH_2$-6-$HOCH_2C_5H_3N$)$Fe(CO)_2X$] (**5**, X = Br; **6**, X = I). Finally complexes **5** and **6** were treated with KSCOMe in MeCN to give the final model complex [(2-$COCH_2$-6-$HOCH_2C_5H_3N$)$Fe(CO)_2$(SCOMe)] **(1)** via replacement of bromide or iodide in **5** and **6** by $MeCOS^-$, so as to resemble the active site with the presence of sulfur in the coordination sphere.

The complex formation was monitored by *in situ* IR spectroscopy. There are significant changes in the ν_{CO} absorption bands versus the starting material $Na_2[Fe(CO)_4]$, intermediate complex **4** (which was too unstable to be isolated), and product **6**. $Na_2[Fe(CO)_4]$ in MeCN has ν_{CO} absorption bands at 1760 (vs), 1866 (w), 1886 (m), and 1915 (w) cm^{-1} gradually diminished, and after 10 min upon the addition 2-(4-$MeC_6H_4SO_3CH_2$)-6-$HOCH_2C_5H_3N$, which indicates the completion of the reaction with the formation of complex **4**. The newly formed complex **4** has a very strong band at 1885 cm^{-1} and a middle band at 2001 cm^{-1}. The formation of complex **6** upon the addition of I_2 exhibits a strong band at 2030 cm^{-1}, a medium band at 1967 cm^{-1}, and a weak band at 1671 cm^{-1} which can be assigned to the two *cis*-oriented terminal carbonyl ligands and one acyl ligand replacing the prior mentioned absorption bands of complex **4**.

Complexes **5-7** were structurally characterized by elemental analysis, spectroscopy, and X-ray crystallography. The geometric comparison of complex **7** to that of the active site shown above shows that the model complex matches the active site parameters very closely. The weakly coordinated hydroxyl group structurally mimics not only the hydroxyl group on the pyridine of the active site but also the H_2O, which is at the 6-

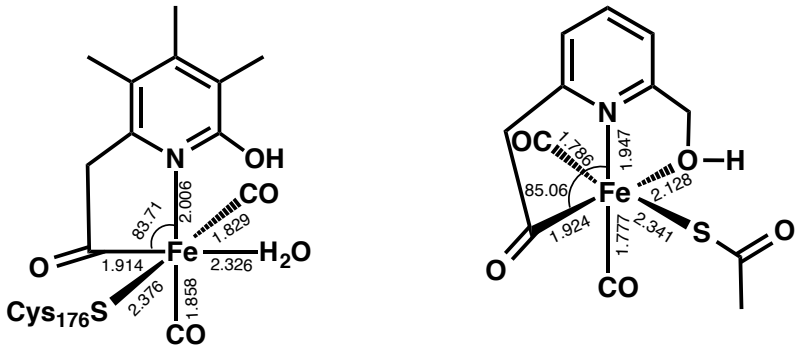

Figure I.6 Geometric parameters for the natural enzyme with FeGP-cofactor (left) and model (right): distance in Å, angles in °.

coordinating position. Thus complexes **5-7** will contribute in further understanding the catalytic mechanism of the active site.

Reversible Dimerization of Mononuclear Models of [Fe]-Hydrogenase[3]

Novel Fe-Hydrogenase models were synthesized via five-coordinate and dimer complexes. This work by Xile Hu *et al*. is the continuation of a previously reported

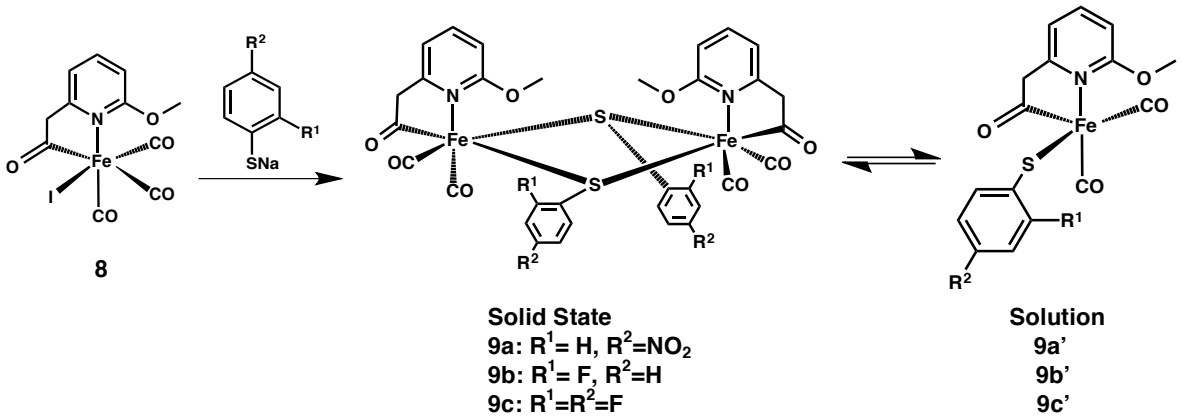

Scheme I.5 Reactions of **8** with sodium aryl thiolate.

five-coordinate complex synthesized by his group. Interestingly, this complex contains an open coordination site which does did not react with H_2 under ambient conditions. This work describes the equilibrium between the dimeric and monomeric complexes. Scheme I.5 gives the reaction of [Fe (2-CH_2CO-6-$MeOC_5H_3N$)$(CO)_3$I] **(8)** with (4-NO_2-C_6H_4)SNa results in a dinuclear complex [{Fe(2-CH_2CO-6-$MeOC_5H_3N$)$(CO)_2${S-(4-NO_2-C_6H_4)}}$_2$] **(9a)** which was characterized by IR spectroscopy, X-ray crystallography in the solid state and NMR spectroscopy in solution. Similar reaction was carried out with various substitutes R^1 and R^2 to yield complexes **9b** and **9c**. These three complexes **9a**, **9b** and **9c** exist as monomeric complexes in solution **9a'**, **9b'** and **9c'**. In the presence of CO a new *tris*(carbonyl) complex [Fe(2-CH_2CO-6-$MeOC_5H_3N$)$(CO)_3${S-(4-NO_2-C_6H_4)}] **(10a)** is formed (Scheme I.6).

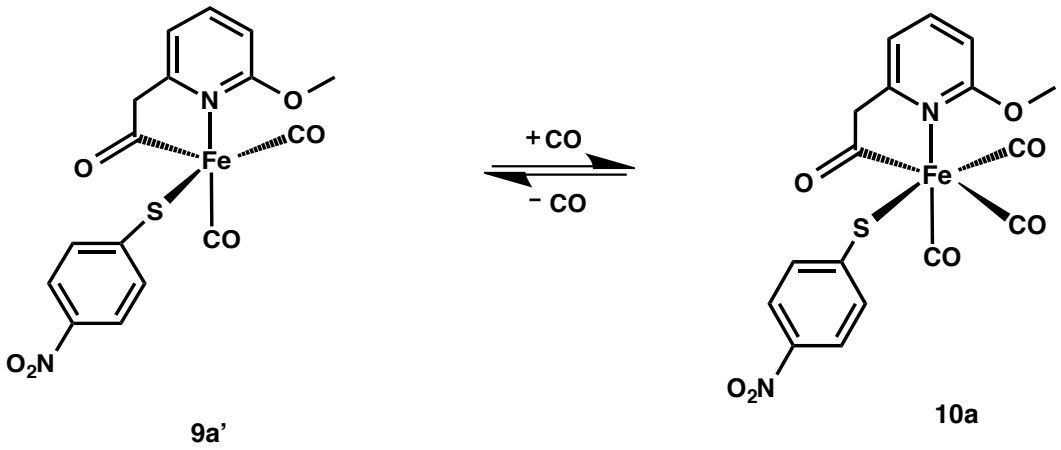

9a' **10a**

Scheme I.6 Reaction of **9a'** with CO.

Further reaction to isolate similar products like **9a'** was carried out (Scheme I.7). Reaction of (2-CF_3-C_6H_4)SNa with complex **8** results in the formation of [Fe(2-CH_2CO-6-$MeOC_5H_3N$)$(CO)_2${S-(2-CF_3-C_6H_4)}] **(9d')** and [Fe(2-CH_2CO-6-$MeOC_5H_3N$)$(CO)_3${S-(2-CF_3-C_6H_4)}] **(10d)**.

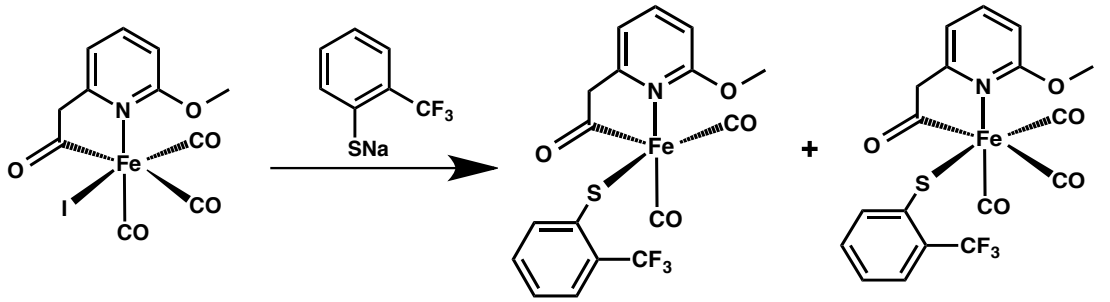

8 **9d'** **10d**

Scheme I.7 Reaction of **8** with (2-CF_3-C_6H_4)SNa.

These complexes have been characterized using NMR spectroscopy. The ratio of **9d'** to **10d** was 5:4 at -30°C. The two complexes are involved in a fast exchange reaction with the transfer of CO.

To isolate pure **9d'** an alternative route (Scheme I.8) was attempted which involved the reaction of $[Fe(2\text{-}CH_2CO\text{-}6\text{-}MeOC_5H_3N)(CO)_2(CH_3CN)_2]BF_4$ **(11)** with $(2\text{-}CF_3C_6H_4)SH$ in the presence of NEt_3 at -30°C which yielded **9d'**. The solution of **9d'** has a half-life of 0.5 h.

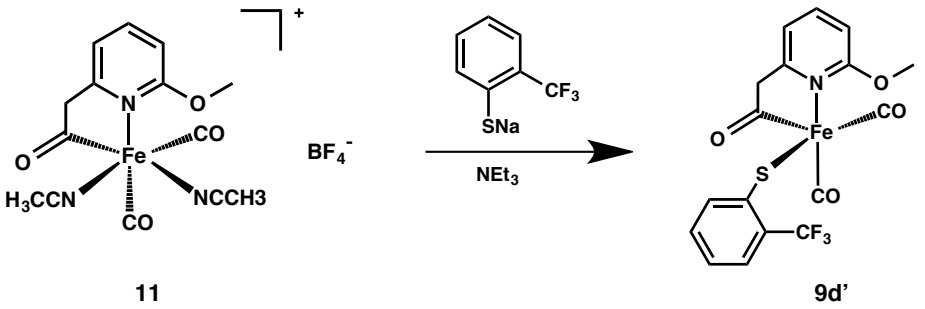

Scheme I.8 Reaction of **11** with $(2\text{-}CF_3\text{-}C_6H_4)SH$ and NEt_3.

A similar reaction was carried out to synthesize **9e**, $[\{Fe(2\text{-}CH_2CO\text{-}6\text{-}MeOC_5H_3N)(CO)_2\{S\text{-}(tBu)\}\}_2]$. This complex which is unstable even at -30 °C in solution yielding **9e'** was characterized only by IR and NMR spectroscopies. The following Scheme I.9 illustrates its synthesis.

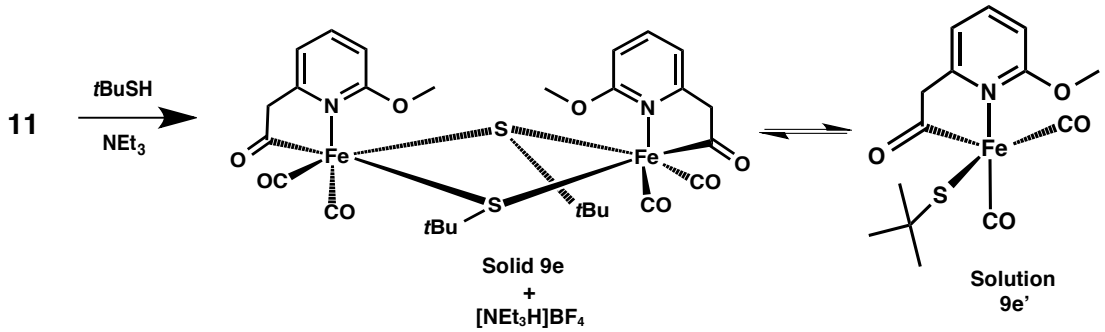

Scheme I.9 Reactions of **11** with tBuSH and NEt_3.

Notably, complexes **9a'**- **9e'** still do not react with H_2 under ambient conditions. It is proposed that the 2-hydroxyl group in the pyridyl ring of the active site of [Fe]-

hydrogenase may play a very important role. Thus, these complexes serve a limited role as reactivity models of [Fe]-hydrogenase.

Synthesis and Reactivity of Mononuclear Iron Models of [Fe]-Hydrogenase that Contain an Acylmethylpyridinol Ligand[4]

Xile Hu *et al*. have also reported mono-iron centered complexes, which model the [Fe]-Hydrogenase with ligated by an acylmethylpyridinol ligand. Complex **12** was prepared by the reaction of [(2-CH_2CO-6-*t*$BuOC_5H_3N$)$Fe(CO)_3I$] with the dropwise addition of lithiated 2-tert-butoxy-6-methylpyridine to [$Fe(CO)_5$], followed by treatment of I_2. The resulting complex **12** is further reacted with NaS(2,6-$Me_2C_6H_3$) to yield a five-coordinate complex [2-CH_2CO-6-t$BuOC_5H_3N$)$Fe(CO)_2${S-(2,6-Me_2-C_6H_3)}] **(13)**.

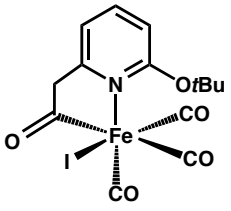

12

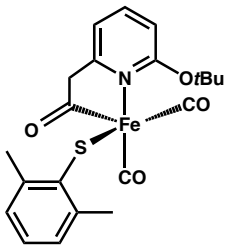

13

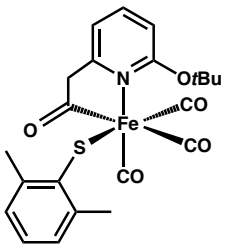

14

Figure I.7 Complexes **12**, **13** and **14**.

Complex **13** was structurally characterized by X-ray crystallography. This complex also shows absence of reactivity in the presence of H_2, which was monitored by NMR spectroscopy. However, the sixth coordination site can be occupied by a third CO ligand resulting is the formation of a new complex **14**, [2-CH_2CO-6-

tBuOC$_5$H$_3$N)Fe(CO)$_3${S-(2,6-Me$_2$-C$_6$H$_3$)}]. This CO in complex **14** is labile in the presence of N_2, regenerating complex **13** (Figure I.7).

Complex **13** was further treated with CF_3COOH/CH_3CN to give a six-coordinate ionic complex (Figure I.8), [(2-CH_2CO-6-tBuOC$_5$H$_3$N)Fe(CO)$_2$(CH$_3$CN)$_2$]$^+$(CF$_3$COO)$^-$ (**15**) which was characterized by NMR and elemental analysis.

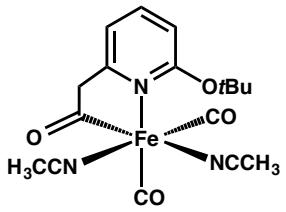

15

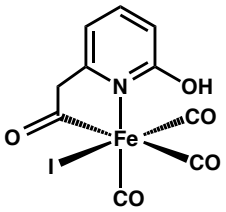

16

Figure I.8 Complexes **15** and **16**.

Deprotection of the *t*Bu group in complex **13** is difficult due to the instable product formed. Therefore a new route to deprotect the *t*Bu group in complex **12** was sought. The reaction of **12** with an excess of Me_3SiI (3.5 equiv) followed by the addition of H_2O resulted in the formation of complex **16** (Figure I.8), [(2-CH_2CO-6-HOC$_5$H$_3$N)Fe(CO)$_3$I], which was characterized by IR and NMR spectroscopies.

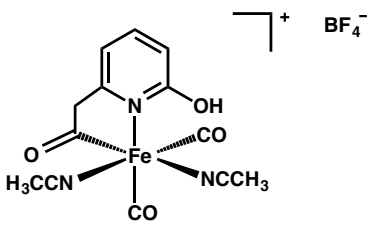

17

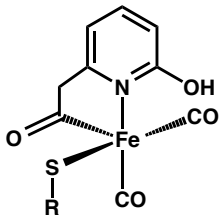

18:R = 2,6 $Me_2C_6H_3$
19:R = 4$NO_2C_6H_4$
20: R = C_6F_6
21:R = *t*Bu
22:R = $CH_2CH_2CH_3$

Figure I.9 Complexes **17**-**22**.

Complex **17** was prepared by the treatment of **16** with $AgBF_4$ in CH_3CN, giving $[(2\text{-}CH_2CO\text{-}6\text{-}HOC_5H_3N)Fe(CO)_2\text{-}(CH_3CN)_2][BF_4]$, (**17**). This complex gave two intense ν_{CO} peaks in IR spectra (in both solid and solution in CH_3CN). Further reaction using this complex by treating **17** with a series of thiols and thiophenols in the presence of NEt_3 at –30 °C to give the targeted thiolate complexes **18**-**22** (Figure I.9). Complexes **18**, **19**, **21** and **22** were only identified using IR spectroscopy as they were too unstable in solution at –30°C to obtain an NMR spectrum. Reaction of complex **20** with H_2, monitored by NMR did not show any reaction. This result is possibly consistent with the essential role of methenyl-H_4MPT^+ for H_2 activation by [Fe]-hydrogenase. In the presence of CO, conversion of **18** and **20** to tricarbonyl complexes $[(2\text{-}CH_2CO\text{-}6\text{-}HOC_5H_3N)Fe(CO)_3\{S\text{-}(2,6\text{-}Me_2\text{-}C_6H_3)\}]$ (**18a)** and $[(2\text{-}CH_2CO\text{-}6\text{-}HOC_5H_3N)Fe(CO)_3\{S\text{-}(C_6F_5)\}]$ (**20a**), Figure I.10, was not complete (33% for **18** and 38% for **20**).

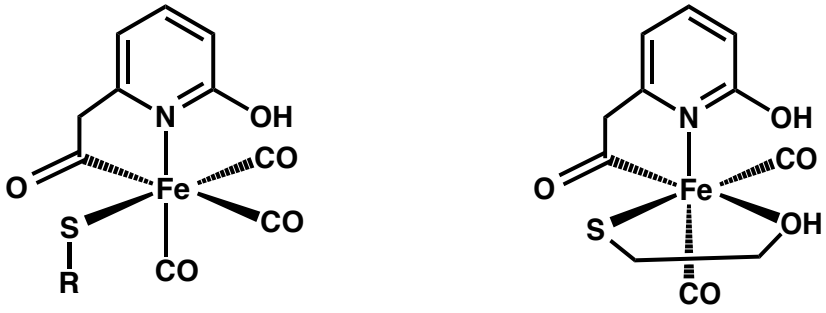

18a:R = 2,6-Me_2-C_6H_3
20a:R = C_6F_5

23

Figure I.10 Complexes **18a**, **20a** and **23**.

When **17** was treated with 2-mercaptoethanol in the presence of NEt_3, [(2-CH_2CO-6-HOC_5H_3N)$Fe(CO)_2(SCH_2CH_2OH)$] (**23**) was produced. The complex was characterized by IR spectroscopy.

To model the acetic acid extracted FeGP cofactor complex **16** was treated with CH_3COOAg in CH_2Cl_2. This yielded complex **24**, which in the presence of CH_3CN exists in equilibrium with **24a** in the ratio of 2:1 (Figure I.11).

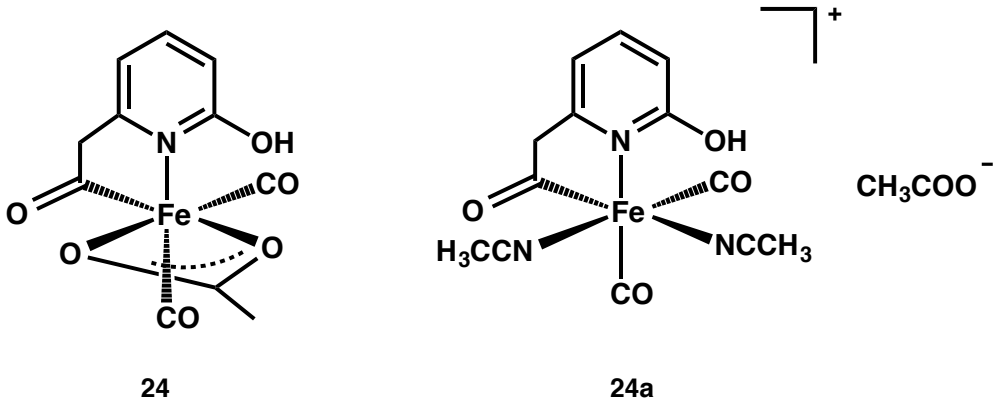

Figure I.11 Complexes **24** and **24a.**

The reaction of **24** with C_6F_5SH/NEt_3 in CH_2Cl_2 results in the five coordinate complex **20**. The same reaction in the presence of 20 equivalents of CH_3CN was carried resulting in the same product **20** this indicates that it exists only as a five coordinate as the iron center does not bind CH_3CN. The lack of reactivity of these new complexes with H_2 suggests that in nature [Fe]-Hydrogenase possibly requires the presence of methenyl-H_4MPT^+ and enzymatic environment for H_2 activation.

2.2. References:

1. Turrell, P. J.; Hill, A. D.; Ibrahim, S. K.; Wright, J. A.; Pickett, C. J. *Dalton Trans*. **2013**, *42*, 8140.
2. Song, L.-C.; Xie, Z.-J.; Wang, M.-M.; Zhao, G.-Y.; Song, H.-B. *Inorg. Chem*. **2012**, *51*, 7466.
3. Hu, B.; Chen, D.; Hu, X. *Chem. Eur. J*. **2013**, *19*, 6221.
4. Hu, B.; Chen, D.; Hu, X. *Chem. Eur. J*. **2014**, *20*, 1.

Scope of the present work

There has been notable interest in synthetic modeling of the active site of [Fe]-Hydrogenase in the past decade. The available synthetic models have a few of the following characteristics.

- The iron source for these complexes initially is in the Fe(0) state, which is then oxidized to Fe(II) during the course of the reaction. However in biology it is likely that the only source of iron is present in the +2 oxidation state.
- In order to make the acyl unit a strong base (e.g. *n*-BuLi) is used to abstract a proton. Therefore it is still not clear how the acyl unit is made in nature, as there are no similarly strong bases in biology.
- The use of a primary amine ($R\text{-}NH_2$) group to make the carbomoyl linkage, even though structurally similar to the active site, does not give insight into the bond formation mechanism of the acyl unit.

Objectives:

The objectives of this study are to make models of the apo-active site replicating some of the characteristics observed in biology as follows:

- To make Hmd Apo-active site model complexes using Fe(II) as the metal site. This is achieved using $[Fe(CO)_4Br_2]$ as the source for both iron and carbonyls.
- To use ligands designed to facilitate the formation of the acyl unit with the addition of milder and more biologically relevant bases.

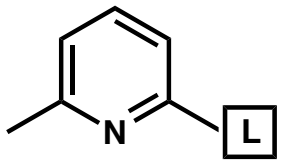

6-methyl-pyridine ligands

2-methyl-pyridine ligands can be a good tool to explore the role of methyl group at the 6-position of the pyridine and then this group will facilitate making the acyl unit.

- To structurally characterize theses complexes using X-ray crystallography.
- To study the stability of the complex using UV-vis and IR spectroscopy.

II. Results and Discussion

Synthesis and X-ray Structures

Metallation reactions using $[Fe(CO)_4Br_2]$ and the un-substituted NNS ligand (i.e. $_HNNS$) were preformed in THF, MeCN and also 1:2 combination of THF/MeCN. Care was taken to eliminate oxidation and therefore these reactions were done in N_2 atmosphere. Reactions were done with and without the presence of $AgBF_4$ to study the influence of the coordinating and non-coordinating counter ion on the formation of the desired product. The desired products of these reactions were the dicarbonyl iron complexes, $[Fe(_HNNS)(CO)_2Br]X$, X = Br, BF_4. The result of the above two reactions (both in the presence and absence of $AgBF_4$) resulted in a purple colored complex, which was later characterized using X-ray crystallography (Figure II.1).

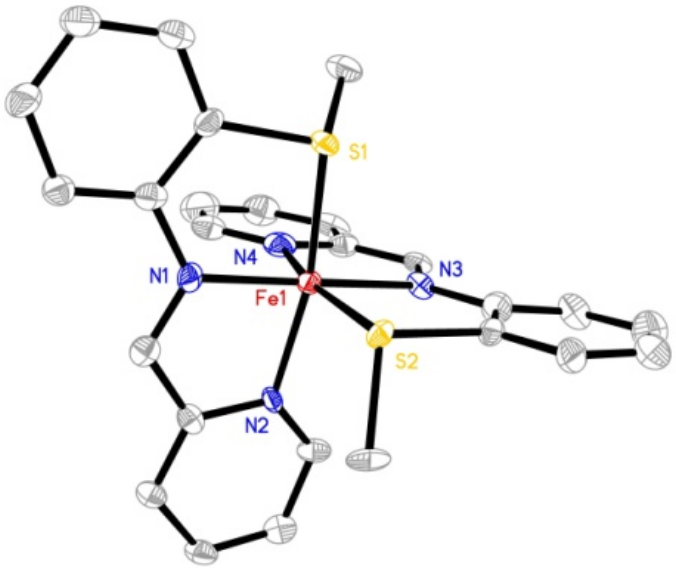

Figure II.1 ORTEP diagrams (50% ellipsoids) of the dication of the *bis*-ligated complex $[(_HNNS)_2Fe](BF_4)_2$.

This neutral, diamagnetic complex has an Fe(II) center and two $_{H}$NNS occupying all the coordinating sites around the metal center with two BF_4 units acting as the counterions. This complex was also characterized in solution state to monitor its stability using ^{1}H NMR (Figure IV.4.). Similar complexes have since been prepared using different substituents on the NNS ligands. Stability studies of these complexes have led us to believe that the choice of solvents and the reaction temperature may have a major effect on the outcome of the product.

Two different reaction conditions were then chosen to bring about the synthesis of the desired product, [Fe($_{H}$NNS)$(CO)_2$Br]X. First, a non-coordinating solvent, Et_2O, was chosen which could completely dissolve both the starting metal complex (the stability of the starting salt was also tested in ether, the carbonyl peaks were retained in solution as in the solid state) and all of the $_{R}$NNS ligand. These reactions were performed under ambient atmosphere and at room temperature. The second set of conditions involved using DCM with or without the coordinating solvent, MeCN, in the ratio of 5:1 at low temperatures (−70 °C) to prevent the loss of CO ligands from the complex.

Reactions in Et_2O

The first metalation reactions in ether were tried using the $_{H}$NNS and $_{H}$NN$_{Me}$S resulting in the formation of dark precipitate, green and brown respectively, in each case, which could not be characterized by X-ray crystallography. Other $_{R}$NNS ligands (R = Me, MeO, PhCl) yielded an orange/green precipitate, which had three carbonyl stretches.

The crystal structures of these complexes revealed that they were dicarbonyl mono-iron complexes with a $[Fe(CO)_3Br_3]^-$ counterion (Shown in Figure IV.2).

1)

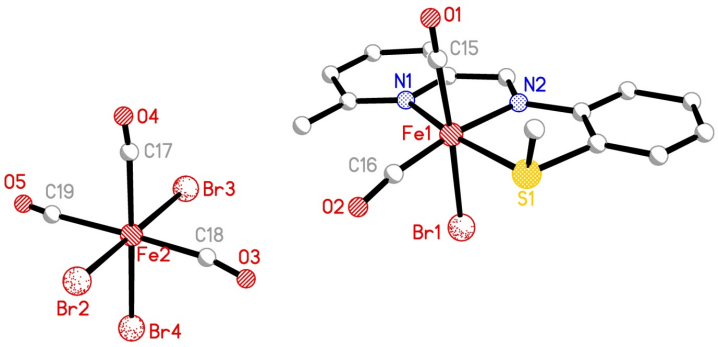

2)

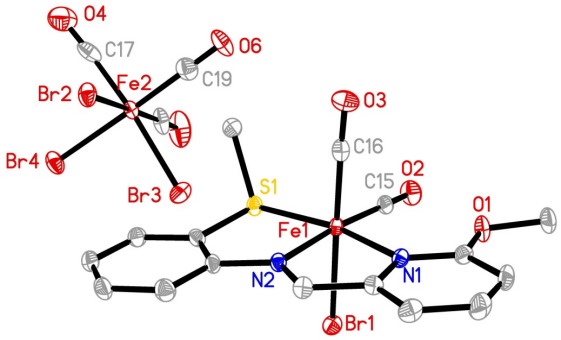

3)

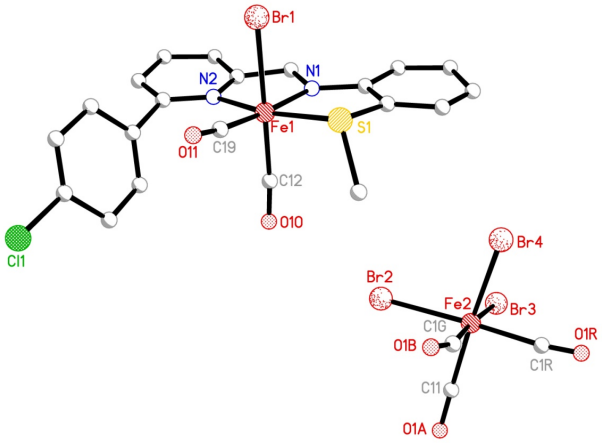

Figure II.2 Crystal structure and connectivity of **(1)** $[(_{Me}NNS)Fe(CO)_3(Br)][Fe(CO)_3(Br)_3]$, **(2)** $[(_{OMe}NNS)Fe(CO)_2Br]$ $[Fe(CO)_3(Br)_3]$ and **(3)** $[(_{PhCl}NNS)Fe(CO)_2Br]$ $[Fe(CO)_3(Br)_3]$.

The above shown complexes had high disorder (**1** and **3**) in the crystal structure due to the counterion. Complex **3** (Figure II.3) was also derived with another counterion $[(_{PhCl}NNS)Fe(CO)_2Br][Fe(Br)_4]$ (**3a**).

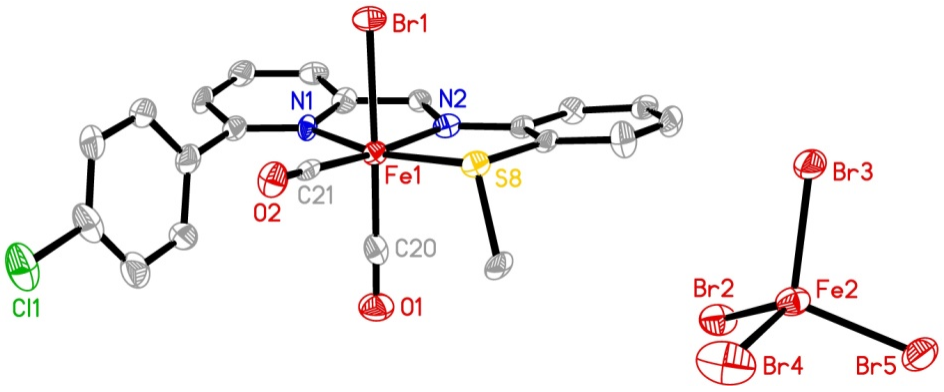

Figure II.3 ORTEP diagrams (50% ellipsoids) of the complex species $[(_{PhCl}NNS)Fe(CO)_2Br][Fe(Br)_4]$ **(3a)**.

The change in the counter ion from the structure $[Fe(CO)_3Br_3]^-$ to $[FeBr_4]^-$ is believed to have occurred because of the storage of the crystals at room temperature. This change was gradual (1 week) and very slow resulting in the loss of CO from the counter ion and oxidation of Fe(II) to Fe(III).

Reactions in DCM/MeCN

Reactions using the second set of conditions (low temperature and DCM/MeCN) yielded the dicarbonyl complexes with bromide as the counter ion in two cases, when $_RNNS$ R = Me and MeO (Figure II.4). When bulkier substituent (R = PhCl, Q) were used the resulting product had $[Fe(CO)_3Br_3]^-$ as the counterion, suggesting that in the case of

bulkier R groups the iron tricarbonyl counter ion has higher stability as compared to the bromide. Reaction using the $_{H}$NNS under this second set of conditions did not yield any product that could be characterized by X-ray crystallography. Product from the reaction of $_{H}N_{Me}NS$ yielded very few crystals, which were characterized using X-ray crystallography.

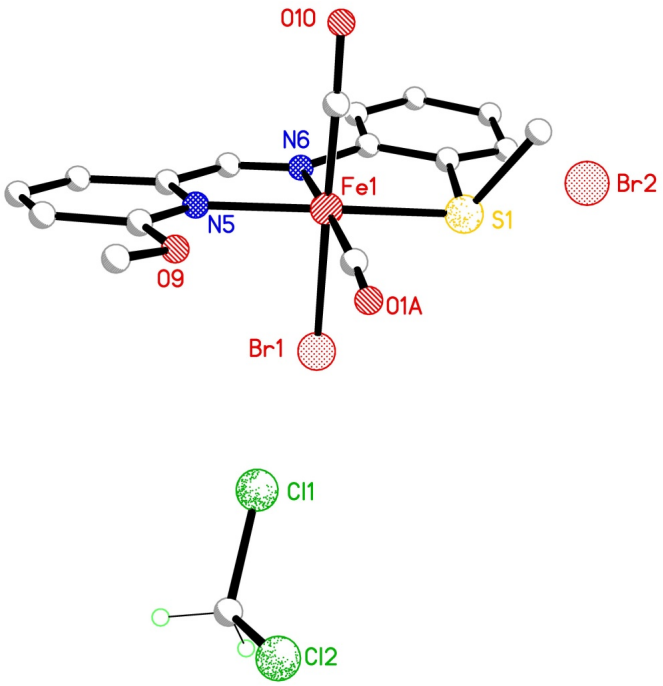

Figure II.4 Connectivity structure of $[(_{OMe}NNS)Fe(CO)_2Br](Br).CH_2Cl_2$.

All of the above-mentioned diamagnetic complexes were characterized using ^{1}H NMR and IR spectroscopies. The preference of one counterion to another in the low temperature DCM/MeCN reactions maybe attributed to the bulkiness of the substituents

at the 6-position of the pyridine ring. Scheme II.1 below shows the possible equilibrium between for the formation of the complex with either Br^- or $[Fe(CO)_3Br_3]^-$.

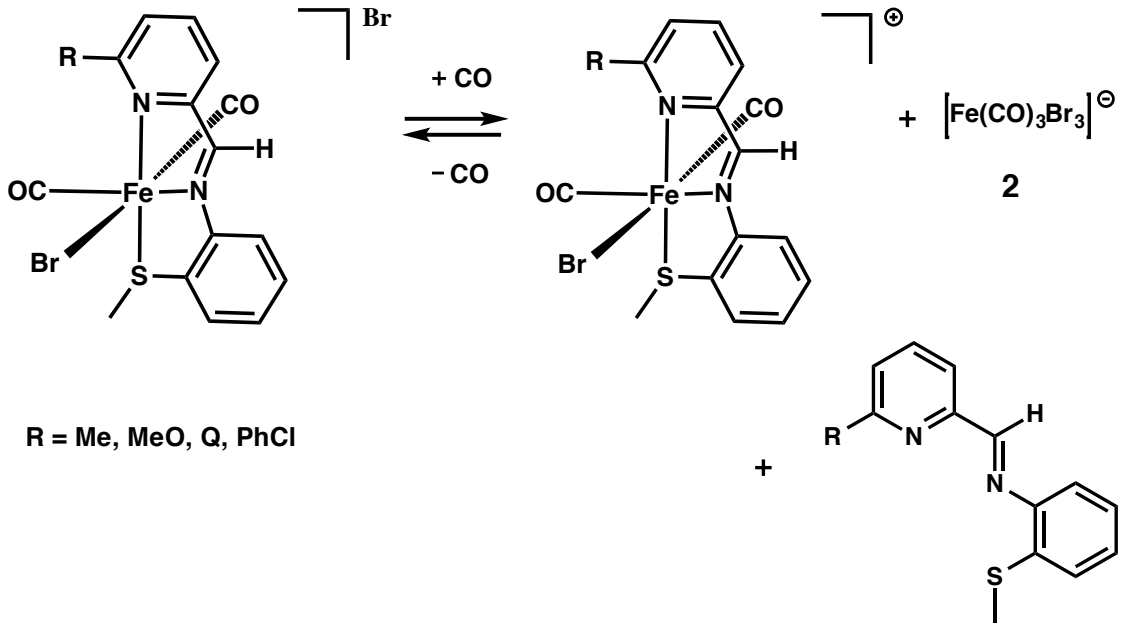

Scheme II.1. Equilibrium in solution for the reaction in DCM/MeCN.

Photolysis of Iron Carbonyl complexes using UV/vis Spectroscopy

In order to assess the influence of the substituents at the sixth position of the pyridine of the dicarbonyl complexes of $[Fe(_RNNS)(CO)_2(Br)][Fe(CO)_3(Br)_3]$, UV/vis spectroscopy was performed. These studies were conducted both in the presence and absence of light at room temperature and under ambient atmosphere. The dicarbonyl iron complexes are stable at very dilute conditions in the absence of light but in the presence of light there was a loss of CO from the complex to form dibromide complexes in solution was observed. Very dilute solutions (0.1 to 1 mM) of the dicarbonyl complexes complex salts with R = Me, OMe, Q and ClPh were prepared in MeCN at low temperature (–30 °C).

1)

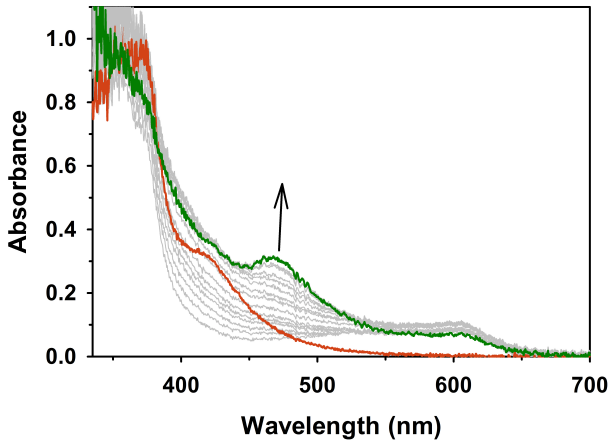

2)

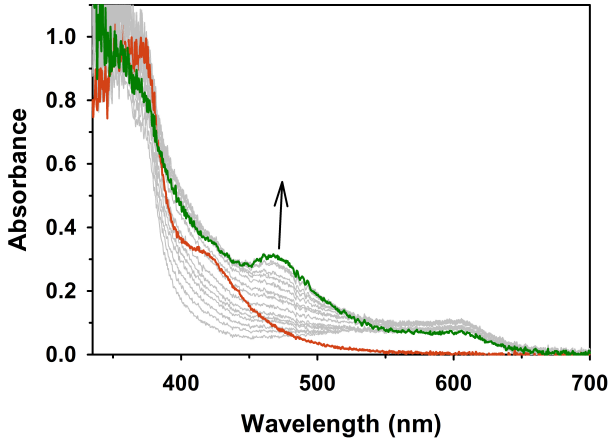

3)

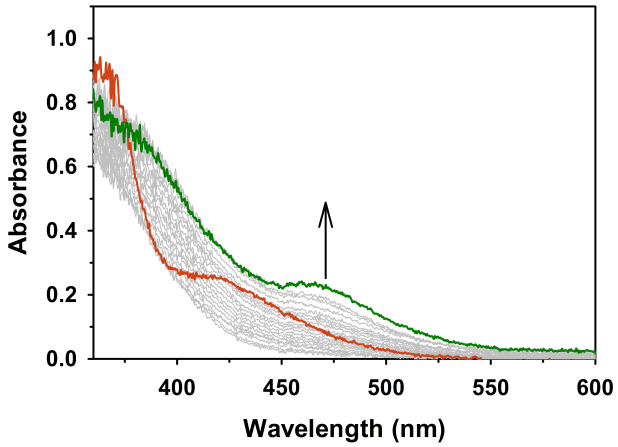

Figure II.5. Changes in UV/vis absorption spectra upon photolysis of $[(_{R}NNS)Fe(CO)_3(Br)][Fe(CO)_3(Br)_3]$, **1)** R= Me**, 2)** R = MeO **3)** R = PhCl with broadband, AM1.5 white light (100 mW/cm^2).

Absorption measurements were preformed at systematic time intervals to follow the increase in the absorbance of the complex at 460 nm, indicating the formation of the dibromides from the dicarbonyl complex with the release of CO (Time vs. Absorbance plots are shown in Figure IV.15. to IV.17.)

The substituents on the 6-position of the pyridine ring effect the photostability of stability with R = OMe being the slowest to lose CO (t½ = 22.6 min) and R = ClPh being the fastest (t½ = 8.5 min), with R= Me (t½ = 12.0 min) appearing moderately stable in comparison. The substituents according to their photostability are OMe > Me > ClPh (Figure II.6). Another type of NNS ligand the $_{Q}$NNS which was also used to make the dicarbonyl complex salts was studied, [[($_{Q}$NNS)Fe(CO)$_3$(Br)][Fe(CO)$_3$(Br)$_3$], whose photostability is comparable with that of the methyl substituted complex (t½ = 12.7 min).

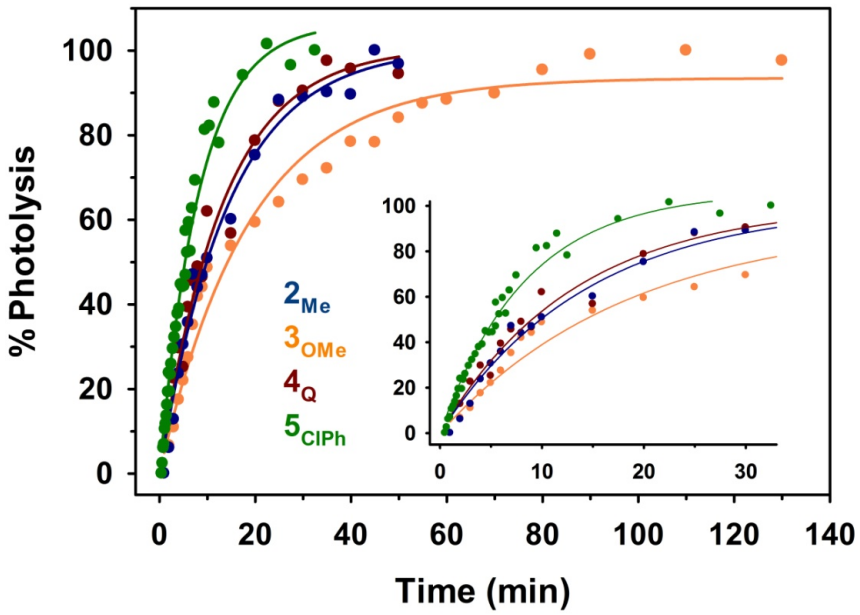

Figure II.6. Photoconversion of the cationic dicarbonyl species (as indicated) to the Fe(II) dibromides via dissociation of CO ligands. *Inset:* Expanded view of the same plot at short time periods. Photolysis conditions: MeCN, 100 mW/cm^2 white light, 298 K.

Since the effect of the counterion on the stability of the complex was unknown, the bromide complex of the methyl-substituted dicarbonyl, $[Fe(_{Me}NNS)(CO)_2(Br)]Br$, was subjected to the same UV/vis studies and conditions stated above. The results were distinct with the iron complex counterion, $[Fe(CO)_3Br_3]^-$, being more sensitive to light of the two different anions, Br^- and $[Fe(CO)_3Br_3]^-$.

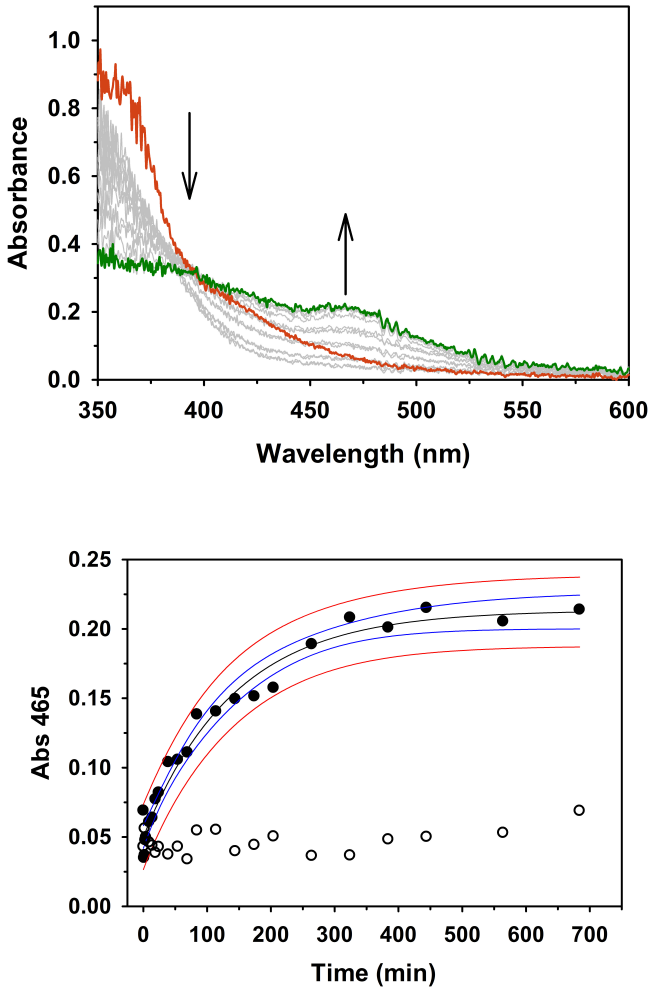

Figure II.7. *Top*: Changes in UV/vis absorption spectra upon photolysis of $[(_{Me}NNS)Fe(CO)_3(Br)]Br$ with broadband, AM1.5 white light (100 mW/cm^2). *Bottom:* Kinetic trace following the absorbance at $\lambda = 460$ nm as indicator of formation of the dibromide species. Blue lines represent the 95% confidence interval of the exponential fit to the data, and red lines represent the 95% prediction band. (Filled Circles – Time intervals in the presence of light. Empty Circles – Time intervals in the absence of light).

Figure II.7 shows that the dicarbonyl complex with the bromide counter ion is much more stable in light (t½ = 128 min) as compared to the same methyl complex with the iron counter ion (t½ = 12.0 min). The reasons for this higher stability may only be attributed to the presence of more available bromide ions for the formation of dibromide in the case of the iron counter ion, $[Fe(CO)_3Br_3]^-$.

Monitoring Photostability of Iron Carbonyls Complexes using Solution IR Spectroscopy

To monitor the loss of CO from the metal center, solution infrared studies were done on $[Fe(_{Me}NNS)(CO)_2(Br)]$ Br. This complex eliminates the interference of the CO groups on the counter ion and has a longer t½, which is preferable since these IR studies were done at much higher concentrations as compared to the UV/vis studies.

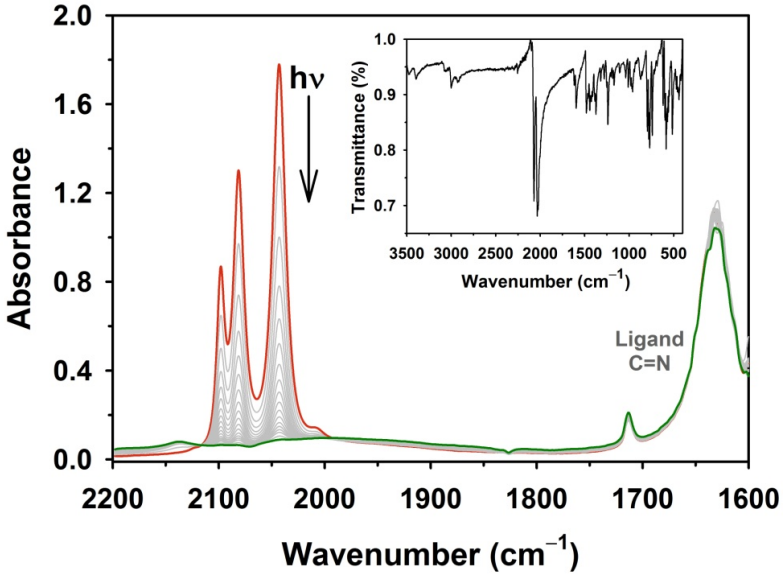

Figure II.8. Solution IR spectra recorded during photoconversion of $[Fe(_{Me}NNS)(CO)_2(Br)]Br$ to $[Fe(_{Me}NNS)(CO)_2(Br)_2]$ in MeCN. Photolysis conditions: ~100 mM, 100 mW/cm^2 white light, 298 K. *Inset:* Solid state IR spectrum of $[Fe(_{Me}NNS)(CO)_2(Br)]$ Br

The figure above (Figure II.8) shows the slow systematic loss of CO from the complex. The figure shows changes in the CO concentration (at 2100-2000 cm^{-1}) of the complex while the Schiff base (at 1500 cm^{-1}) of the ligand is intact, indicating that the complex is only losing CO ligands with the ligand still bond to the central metal atom.

III. Materials and Methods

General Procedures and Reagents

The starting materials for the preparation of the iron salt and the ligands were obtained from Acros Organics or Sigma Aldrich and were used without further purification. $[Fe(CO)_4Br_2]$ and some of the NNS ligands namely ($_{H}$NNS),($_{Me}$NNS) and ($_{Q}$NNS) were prepared according to literature.[1,2,3,4] These methods have been given in detail below. HPLC grade solvents were purchased from EMD, Fisher, Macron or J.T.Baker, and dried through an alumina column system (Pure Process Technology). Deuterated solvents were purchased from Cambridge Isotopes or Acros Organics.

Characterization of $_{R}$NNS ligands and Iron Carbonyl complexes

All synthesized $_{R}$NNS ligands and complexes were characterized using ^{1}H NMR and solid-state IR spectroscopies. ^{1}H NMR spectra for the ligands were collected on a Varian DirecDrive 400 MHz spectrometer and all chemical shifts were referenced to TMS. High-resolution mass spectroscopy was used in cases where the ligand was obtained as a mixture of the desired product and starting material.

The metal complexes were structurally characterized using X-ray crystallography. The data was collected either on a Rigaku AFC12 diffractometer with a Saturn 724+ CCD or on a Nonius Kappa CCD diffractometer using a Bruker AXS Apex II detector, both using a graphite monochromator with MoKα radiation. Reduced temperatures were maintained using an Oxford Cryostream low temperature device. Data reduction were performed using the Rigaku Crystal Clear version 1.40.2. Structures were solved by

direct methods using SIR973 and refined by full-matrix least-squares on F^2 with anisotropic displacement parameters for the non-H atoms using SHELXL-97.4. Structure analysis was aided by use of the programs PLATON985 and WinGX.6. ^{1}H NMR spectra of the iron carbonyl complexes were recorded on a 500 MHz Varian Inova instrument fitted with a variable temperature apparatus. The stability in solution was also confirmed using ^{1}H NMR spectroscopy at low temperatures (−5 °C ~ −30 °C).

The presence of Schiff bases in the ligands and carbonyls in the metal complexes were confirmed using solid state Infrared spectroscopy (Bruker Alpha spectrometer equipped with a diamond ATR crystal).

Ligand Synthesis

N_{Me}NS. 2-(methylthio)-*N*-(1-(pyridin-2-yl)ethylidene)aniline.

2-(methylthio)aniline (0.500 g, 3.59 mmol) was diluted in 5 mL acetic acid, and to this solution was added 2-acetylpyridine (0.434 g, 3.59 mmol) in 5 mL AcOH. Next, a slurry of $ZnCl_2$ (0.489 g, 3.59 mmol) in 5 mL of AcOH was added, and the reaction refluxed for 1 h to generate an orange solution (when hot). Upon cooling a yellow solid forms, which was collected by filtration and washed with several portions of Et_2O. The solid was then dissolved in CH_2Cl_2 (25 mL) and washed 2× in a separatory funnel with 0.25 M $K_2C_2O_4$, and 2× with water. The organic layer was dried over Na_2SO_4 and evaporated to dryness by rotary evaporation to afford a yellow oil. Yield: 0.49 g (56%). Selected IR bands (ν in cm^{-1}): 3052 w, 2919 w, 1635 s, 1578 m, 1565 m, 1466 s, 1434 s, 1301 m, 993 w, 965 w, 780 vs, 737 vs, 649 w, 621 m. ^{1}H NMR in $CDCl_3$ (δ in ppm from TMS): 8.66 (d, J = 4

Hz, 1H), 8.39 (d, *J* = 8 Hz, 1H), 7.79 (t, *J* = 7.2, 1H), 7.36 (dt, *J* = 6.4 Hz, 1H), 7.25 (d, *J* = 2.4 Hz, 1H), 7.14 (m, 2H), 6.72 (d, *J* = 7.2 Hz, 1H), 2.37 (s, 3H), 2.34 (s, 3H). HRMS calcd: 241.0799, 242.0878, 243.0956; found: 241.0802, 242.0878, 243.0959.

$_{OMe}$NNS. 1-(6-methoxy-2-pyridyl)-*N*-(2-methylsulfanylphenyl)methanimine.

A batch of 6-methoxy-2-pyridinecarboxaldehyde (2.00 g, 14.6 mmol) was dissolved in 20 mL of MeOH. To this stirred solution was added a solution of 2-(methylthio)aniline (2.03 g, 14.6 mmol) in 15 mL of MeOH. The solution was heated to reflux temperature for 2 h, at which point the solution was cooled to ambient temperature and solvent evaporated under a stream of N_2 gas. The resulting tacky solid was gently triturated 2× with Et_2O to yield an orange solid. Selected IR bands (ν in cm^{-1}): 1623 w, 1587 m, 1567 s, 1462 s, 1439 s, 1321 m, 1138 w, 800 vs, 750 vs, 725 vs, 635 w, 538 m. ^{1}H NMR in $CDCl_3$ (d from TMS): 8.44 (s, 1H), 7.90 (d, *J* = 7.2 Hz, 1H), 7.68 (t, *J* = 7.2 Hz, 1H), 7.23 (br, 1H), 7.16 (br, 1H), 7.08 (br, 1H), 6.82 (d, *J* = 8.4 Hz, 1H), 6.75 (br, 1H), 4.00 (s, 3H), 2.47 (s br, 3H). HRMS calcd: 257.0749, 258.0827, 259.0905; found: 257.0756, 258.0833, 259.0903. NMR analysis indicated unreacted (~30%) aldehyde that was not separated by fractional crystallization or chromatography. The mixture was used in subsequent metalations.

$_{ClPh}$N,N,SMe. *N*-((6-(4-chlorophenyl)pyridn-2-yl)methylene)-2-(methylthio)aniline.

6-(4-chlorophenyl)-2-pyridine carboxaldehyde (0.500 g, 2.30 mmol) was suspended in 10 mL of MeOH, upon the addition of a solution of 2-methylthioaniline (0.574 g, 2.30

mmol) in 10 mL of MeOH, the color of the solution changes from colorless to a bright yellow while forming a hazy solution. This mixture was refluxed for 2 h, during which it turned to a clear solution. On being cooled to room temperature, the reaction mixture precipitates the fluffy greenish yellow ligand. The solvent was evaporated using rotavap. The resulting solid was washed with ether (10 mL) to remove excess starting materials to afford a yellow sample of the ligand, analytically pure in the solid state. In the ^{1}H NMR it shows a mixture of ligand peaks and the hydrolyzed product peaks. Yield: 0.64 g (63%). Selected IR bands (ν in cm^{-1}): 1592 m, 1570 m, 1495 m, 1426 m, 1317 w, 1163 m, 1033 s, 930 m, 804 vs, 745 vs, 677 w, 663 w. ^{1}H NMR in $CDCl_3$ (δ in ppm from TMS): 8.67 (s, 1H), 8.29 (d, J = 8 Hz, 1H), 8.01 (d, J = 8.8 Hz, 2H), 7.89 (m, 3H), 7.79 (d, J = 7.6 Hz, 1H), 7.48 (m, 2H), 7.35 (b, 1H), 7.12 (b, 1H), 6.73 (1H), 2.47 (s, 3H).

Synthesis of Metal Complexes

Tetracarbonyldibromoiron(II) [$Fe(CO)_4Br_2$]

In 100 mL DCM, 3 mL (23 mmol) of [$Fe(CO)_5$] was dissolved at RT. This solution was then kept at -40 °C. A solution of Br_2 (1.5 mL, 29 mmol) in 20 mL DCM was taken in a 25 mL Schlenk flask. This was then added drop-wise using a cannula to the [$Fe(CO)_5$] solution. A bright orange precipitate was formed. The reaction mixture was stirred for 1-1.5 h and warmed to RT. The color of the resulting precipitate is red/orange. The solvent was removed using short path/vacuum distillation and a dark red/brown precipitate was collected. This was washed with pentane and was then dissolved in minimal amounts of DCM and recrystallized by vapor diffusion of pentane at −20 °C. The crystals were

characterized by IR spectroscopy. Selected IR bands (ν in cm^{-1}): 2158 cm^{-1}, 2110 cm^{-1}, 2091 cm^{-1} and 2059 cm^{-1}.

$[(_{H}NNS)_2Fe](BF_4)_2$

At room temperature, to a stirred solution of 1 equiv of $_{H}$NNS (100 mg, 0.438 mmol) in 10 mL of MeCN was added 2 mL of THF containing 1 equiv of $[Fe(CO)_4(Br)_2]$ (118 mg, 0.438 mmol). Addition of iron carbonyl immediately generated a dark violet color that was indefinitely stable under ambient conditions. To isolate the BF_4 salt of the complex, 1 equiv of $AgBF_4$ (85 mg, 0.438 mmol) in 2 mL of THF was added; although no color change was observed, a turbid solution was generated (AgBr) and the resulting mixture was stirred overnight, and then filtered twice through Celite. Vapor diffusion of Et_2O at room temperature afforded violet blocks suitable for X-ray diffraction. Yield: 65 mg (21%). Selected IR bands (ν in cm^{-1}): 1604 w, 1585 w, 1477 m, 1306 w, 1162 w, 1029 vs, 916 m, 775 s, 765 s, 750 s, 606 m, 516 s, 417 w. ^{1}H NMR (500 MHz) in CD_3CN, δ from TMS (ppm): 10.18 (s 2H), 8.58 (d, J = 8 Hz, 2H), 8.34 (d, J = 4 Hz, 2H), 8.02 (t, J = 4 Hz, 2H), 7.82 (m, 6H), 7.75 (t, J = 12 Hz, 2H), 7.38 (t, J = 4 Hz, 2H), 2.14 (s, 6H). Elemental Analysis, calcd: C 45.38, H 3.81, N 8.14; found: C 45.29 H 3.77 N 8.27.

General Procedure for $[(_{R}NNS)Fe(CO)_2Br][Fe(CO)_3(Br)_3]$

Iron tetracarbonyl bromide (1 equiv) was dissolved in dry Et_2O to give a bright red solution, which was stirred until homogenous. To this solution was slowly added a solution of the $_{R}$NNS (1 equiv) in dry Et_2O. Upon the addition of the ligand, there was an

immediate color change along with precipitation of the product. This mixture was stirred for 30 min, after which it was filtered and the precipitate was set up for recrystallization in acetonitrile with vapor diffusion of Et_2O at −20°C.

[($_{Me}$NNS)Fe(CO)$_2$Br][Fe(CO)$_3$(Br)$_3$]

(E)-1-(6-methylpyridin-2-yl)-*N*-(2-(methylthio)phenyl)methanimine (50 mg, 0.2065 mmol) in 5 mL Et_2O (yellow solution) was added to a red solution of iron tetracarbonyl bromide (67mg, 0.2065 mmol) in 5 mL Et_2O. An immediate color change to orange-red with the formation of precipitate was observed. The mixture was stirred for 30 min and the crude product was collected by gravity filtration under ambient atmosphere. The resulting precipitate was a blend of orange and green. The product was recrystallized to yield red-orange crystals. Yield: 50 mg (30%). Selected IR bands (ν in cm^{-1}): 2092 m, 2075 s, 2033 vs, 1411 w, 1237 w, 798 m, 773 m, 621 vs, 569 vs, 511.7 s, 442 w. ^{1}H NMR (500 MHz) in CD_3CN at −25°C, δ from TMS (ppm): 9.68 (s, 1H), 8.30 (d, *J* = 4 Hz, 1H), 8.09 (m, 2H), 7.92 (d, *J* = 4 Hz, 1H), 7.82 (t, *J* = 4 Hz, 1H), 7.67 (d, *J* = 4 Hz, 1H), 3.03 (s 3H, $_{py}CH_3$), 2.64 (s 3H, S-CH_3).

[($_{MeO}$NNS)Fe(CO)$_2$Br][Fe(CO)$_3$(Br)$_3$]

(*E*)-1-(6-methoxypyridin-2-yl)-*N*-(2-(methylthio)phenyl)methanimine (50 mg, 0.1935 mmol) was metallated with a solution of iron tetracarbonyl bromide (63 mg, 0.1935 mmol) in 10 mL Et_2O. An immediate color change to orange-red with the formation of precipitate is observed. The mixture was stirred for 30 min and the crude product was

collected by gravity filtration under ambient atmosphere. The resulting precipitate was a blend of orange and green. Recrystallization afforded orange-red rod shaped crystals. Yield 50 mg (31%). Selected IR bands (ν in cm^{-1}): 2095 m, 2081 m, 2032 vs, 1593 w, 1561 w, 1483 m, 1243 w, 1192 w, 797 m, 572 s, 518 m. NMR (500 MHz) in $CDCN_3$ at −5°C, δ from TMS (ppm): 9.66 (s, 1H), 8.32 (br, 1H), 8.21 (br, 1H), 7.82 (br, 1H), 7.75 (t, J = 4 Hz, 1H), 7.67 (d, J = 4 Hz, 1H), 4.22 (s, 3H), 2.64 (s, 3H).

[($_{ClPh}$NNS)Fe(CO)$_2$Br][Fe(CO)$_3$(Br)$_3$]

(*E*)-1-(6-(4-chlorophenyl)pyridin-2-yl)-*N*-(2-(methylthio)phenyl)methanimine (50 mg, 0.1477 mmol) in 5 mL Et_2O was metallated with iron tetracarbonyl bromide (48 mg, 0.1477 mmol) in 5 mL Et_2O. An immediate color change to orange-red with the formation of precipitate is observed. The mixture was stirred for 30 min and the crude product is collected by gravity filtration under ambient atmosphere. The resulting precipitate was a blend of orange powder. The product was recrystallized to yield red-orange crystals. Yield 43 mg (34%). Selected IR bands (ν in cm^{-1}): 2095 m, 2067 m, 2034 s, 2025 vs, 1600 w, 1254 w, 1095 m, 966 w, 760 m, 621 s, 581 s, 437 w. IR bands of the crystallized $[Fe(CO)_3Br_3]^-$ complex : 2092 m, 2070 m, 2033 s, 2025 s, 1614 w, 1253 w, 1094 m, 967 m, 768 m, 619 m, 580 s, 439 w. NMR (500 MHz) in $CDCN_3$ at 5 °C, δ from TMS (ppm): 9.79 (s, 1H), 8.34 (m, 2H), 8.27 (br, 1H), 7.86 (m, 2H), 7.75 (m, 4H), 7.75 (m, 4H), 7.58 (d, J = 4 Hz, 1H), 7.53 (d, J = 4 Hz, 1H), 2.54 (s, 3H).

[($_{MeO}$NNS)Fe(CO)$_2$Br]Br

Iron tetracarbonyl bromide (163 mg, 0.3870 mmol) was dissolved in 3 mL of dry DCM at -75 °C under N_2 atmosphere. A yellow solution of $_{MeO}$NNS (100 mg, 0.3870 mmol) in 3 mL dry DCM was cooled to −75 °C and then transferred through cannula to the above solution. This reaction was stirred for 10 min to yield a green-red solution. On the addition of dry MeCN (3 mL) via cannula, the color of the solution turned clear red. Recrystallization at −25 °C yielded very few crystals with good diffraction and a green-purple precipitate, presumably of the dibromide and the *bis*-ligated complex.

[($_{ClPh}$NNS)FeBr$_2$]

A solution of $_{ClPh}$NNS (50 mg, 0.148 mmol) in 3 mL of dry DCM under N_2 condition is transfer through cannula to a solution of iron tetracarbonyl bromide, [Fe(CO)$_4$Br$_2$], (48 mg, 0.148 mmol) in 3 mL dry DCM kept at −75 °C under N_2 conditions. The color of the reaction mixture changes from red to orange. MeCN (3 mL) is added to this through cannula, which changes the color to red orange. The resulting mixture was kept at −20 °C for several days which resulted in the formation of small amount of green crystals. Selected IR bands (ν in cm^{-1}): 3035 m, 1620 m, 1598 m, 1092 m, 832 s, 811 s, 522 m, 475 m.

Reference:

1. Turrell, P. J.; Wright, J. A.; Peck, J. N. T.; Oganesyan, V. S.; Pickett, C.J. *Angew. Chem. Int. Ed*. **2010**, *49*, 7508.
2. Chatterjee, S. K.; Roy, S.; Barman, S. K.; Maji, R. C.; Olmstead, M. M.; Patra, A. K. *Inorg. Chem*. **2012**, *51*, 7625.
3. Roy, S.; Mitra, P.; Patra , A. K. *Inorg. Chim. Acta*. **2011**, *370*, 247.
4. Lumsden, S. E. A.; Durgaprasad, G.; Thomas Muthiah, K. A.; Rose, M. J.; *Dalton Trans*. **2014**, 10725.

IV. Spectroscopic Data

NMR of NNS Ligands

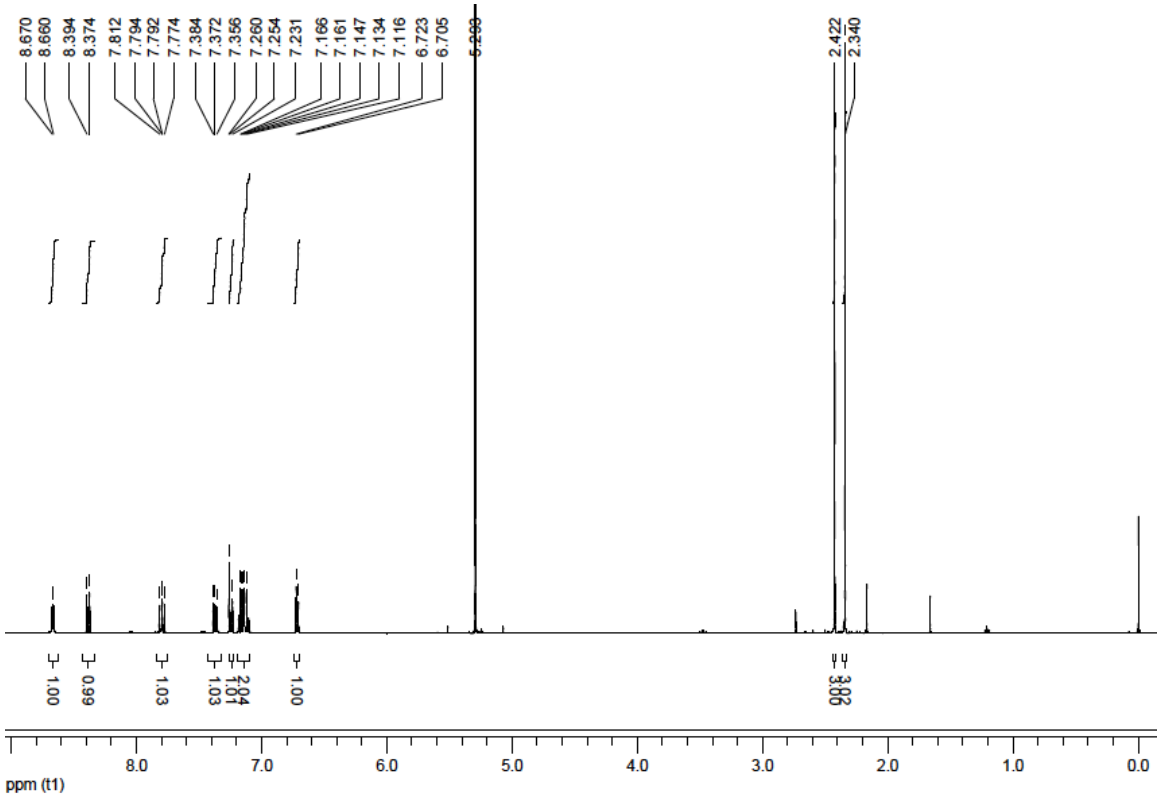

Figure IV.1. ^{1}H NMR spectrum (400 MHz) of $N_{Me}NNS$ obtained in $CDCl_3$ at 25 °C.

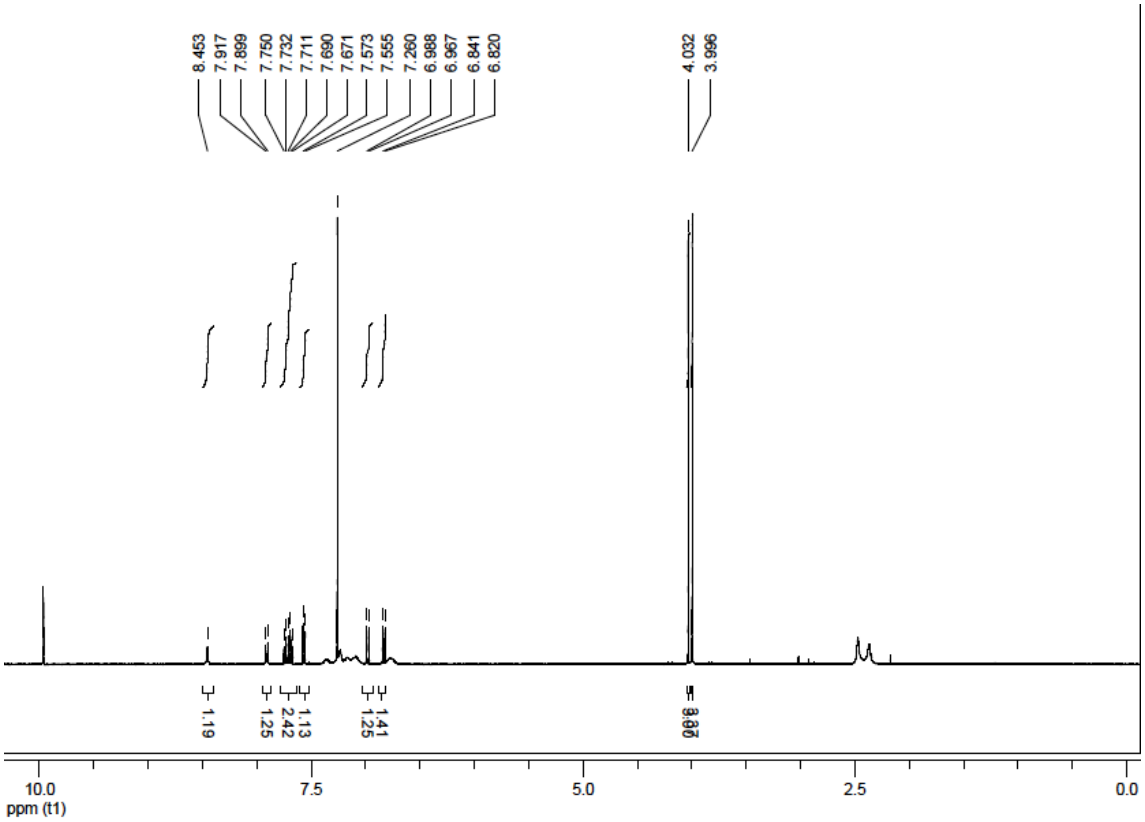

Figure IV.2. ^{1}H NMR spectrum (400 MHz) of $_{MeO}$NNNS obtained in $CDCl_3$ at 25 °C.

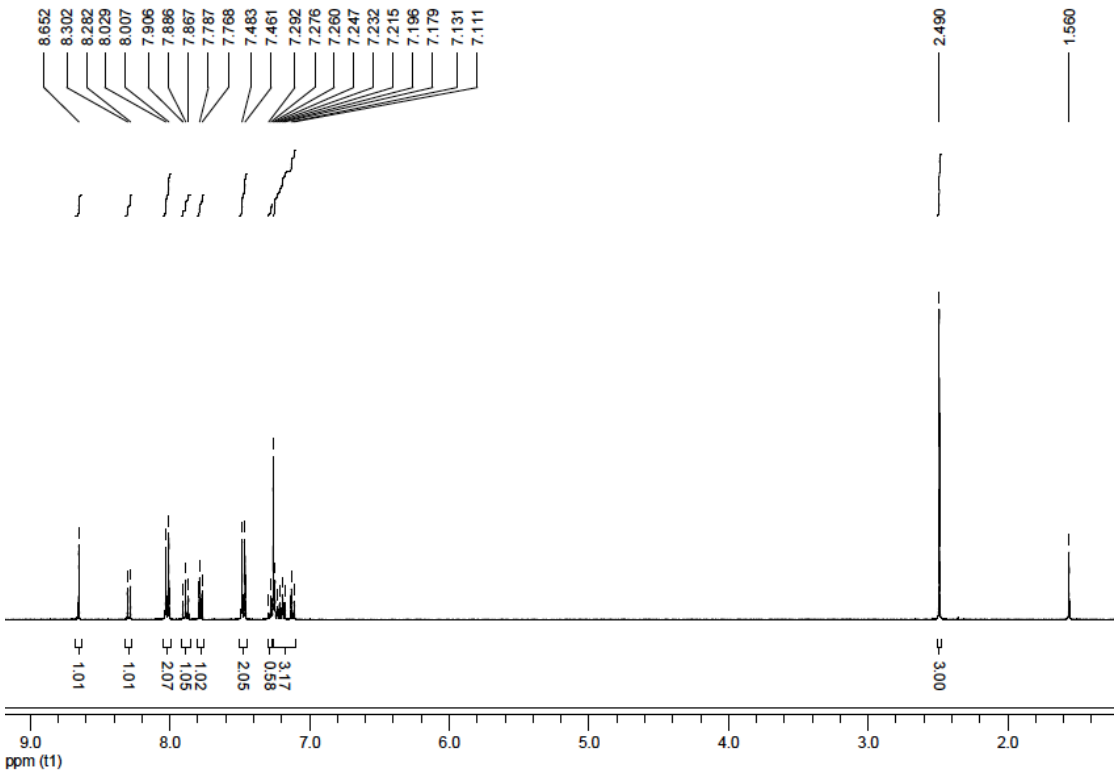

Figure IV.3. ^{1}H NMR spectrum (400 MHz) of $_{PhCl}$NNNS obtained in $CDCl_3$ at 25 °C.

NMR of Iron Complexes

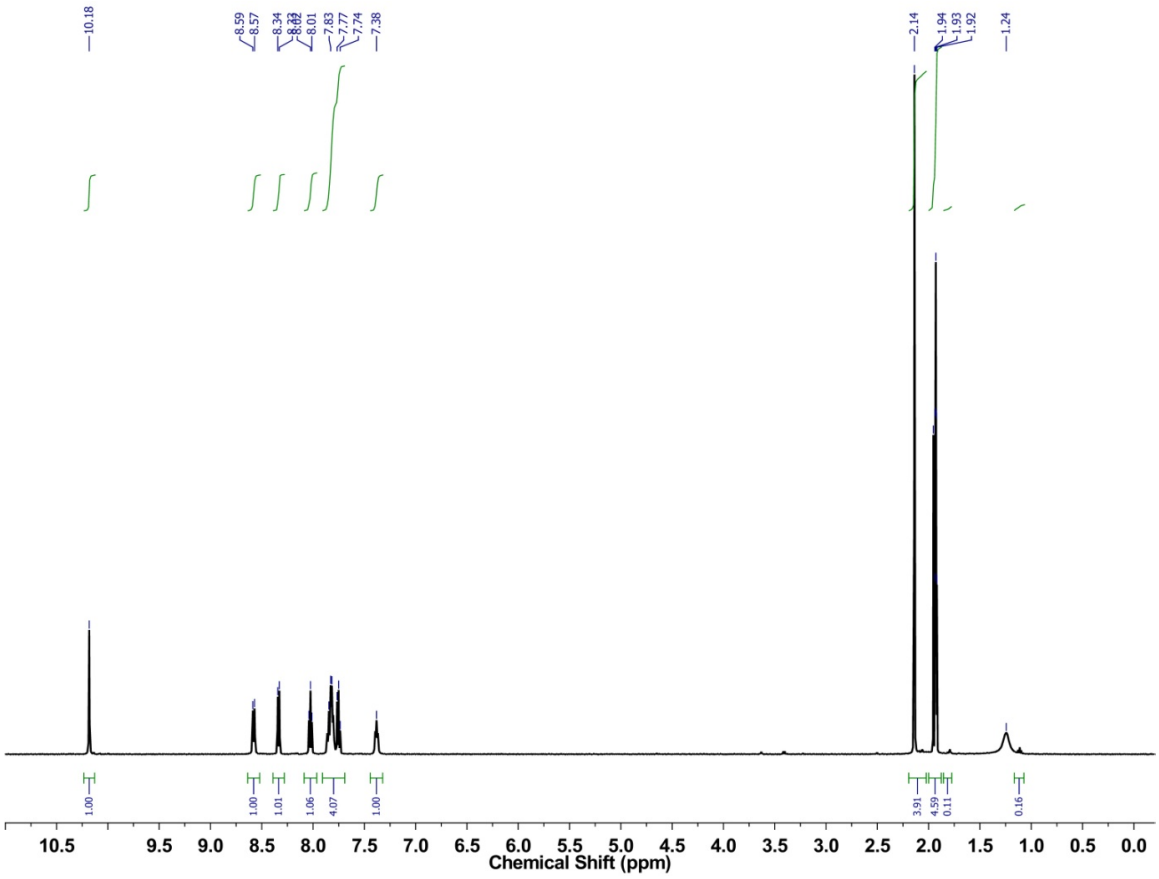

Figure IV.4. ^{1}H NMR spctrum (500 MHz) of $[(_{H}NNS)_2Fe](BF_4)_2$ obtained in CD_3CN at 25 °C.

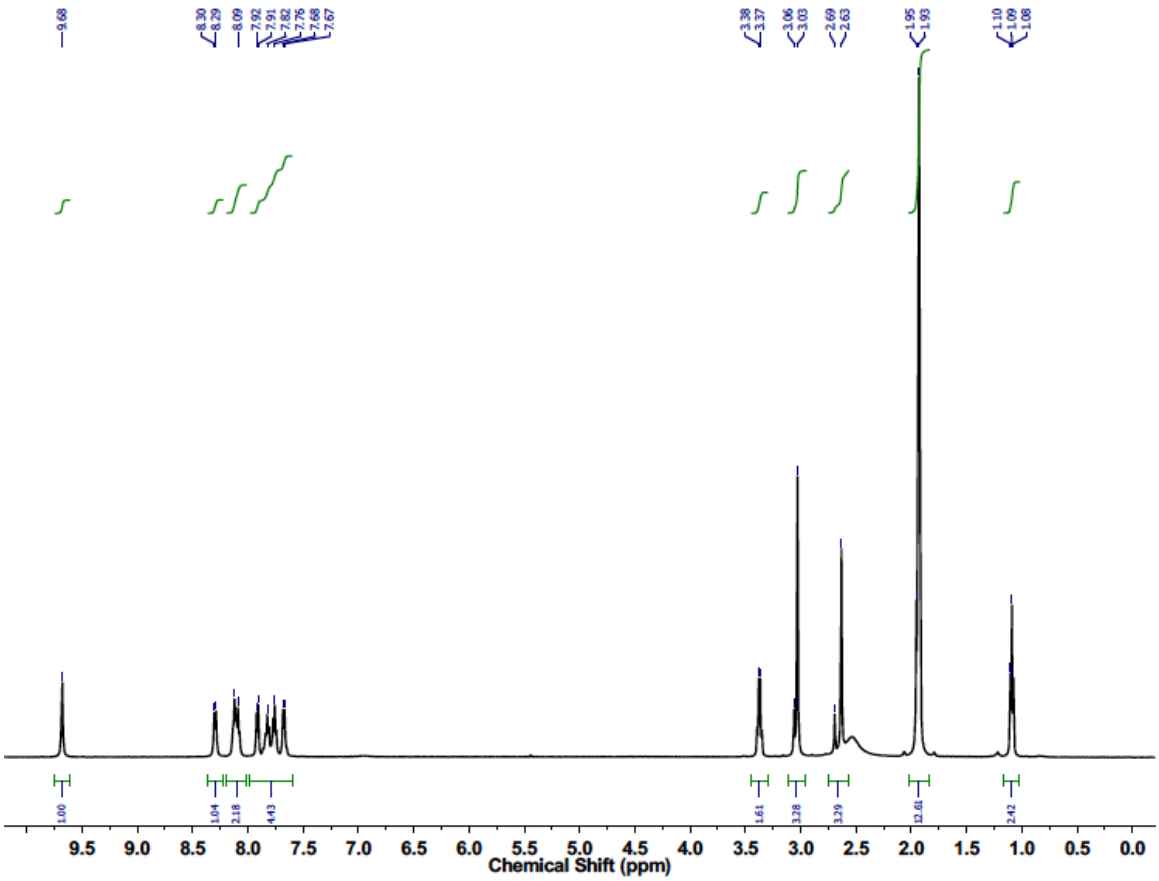

Figure IV.5. ^{1}H NMR spectrum (500 MHz) of $[(_{Me}NNS)Fe(CO)_2Br][Fe(CO)_3(Br)_3]$ obtained in CD_3CN at -25 °C.

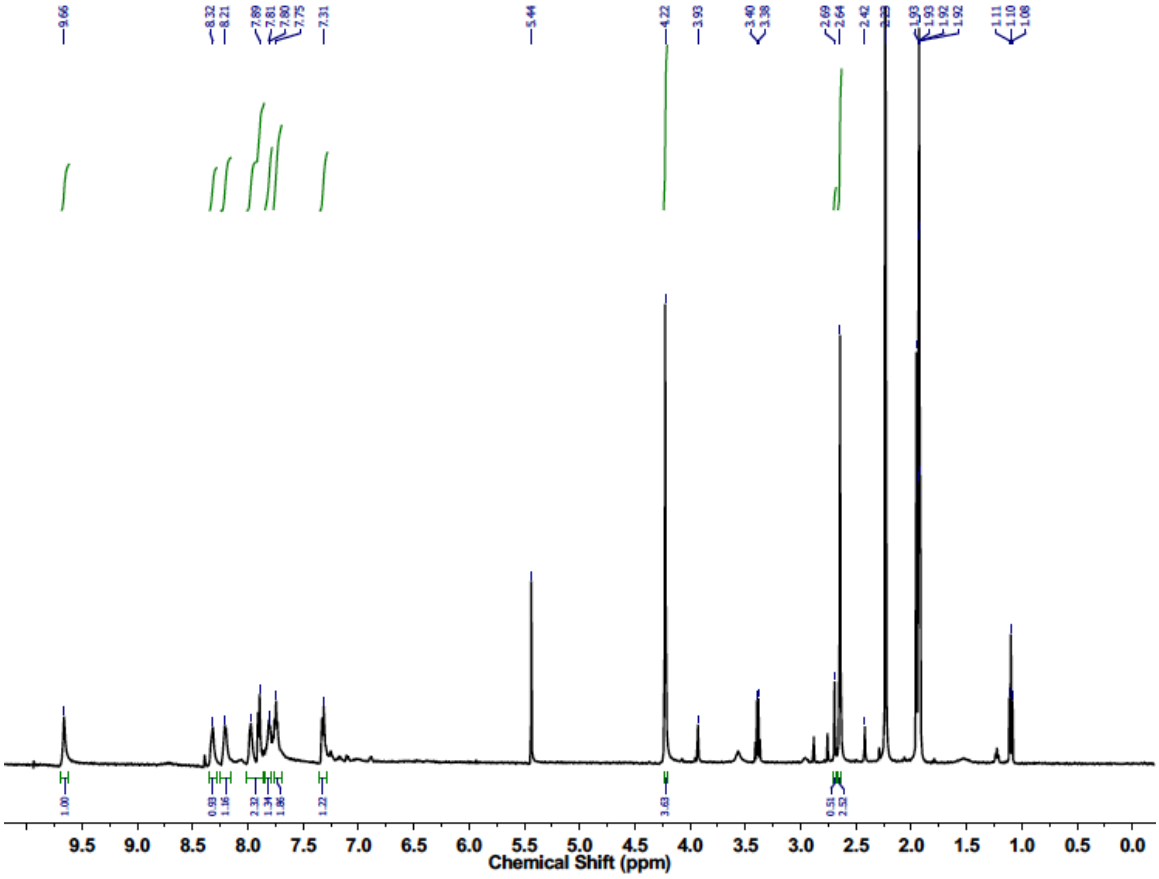

Figure IV.6. ^{1}H NMR spectrum (500 MHz) of $[(_{MeO}NNS)Fe(CO)_2Br][Fe(CO)_3(Br)_3]$ obtained in CD_3CN at -5 °C.

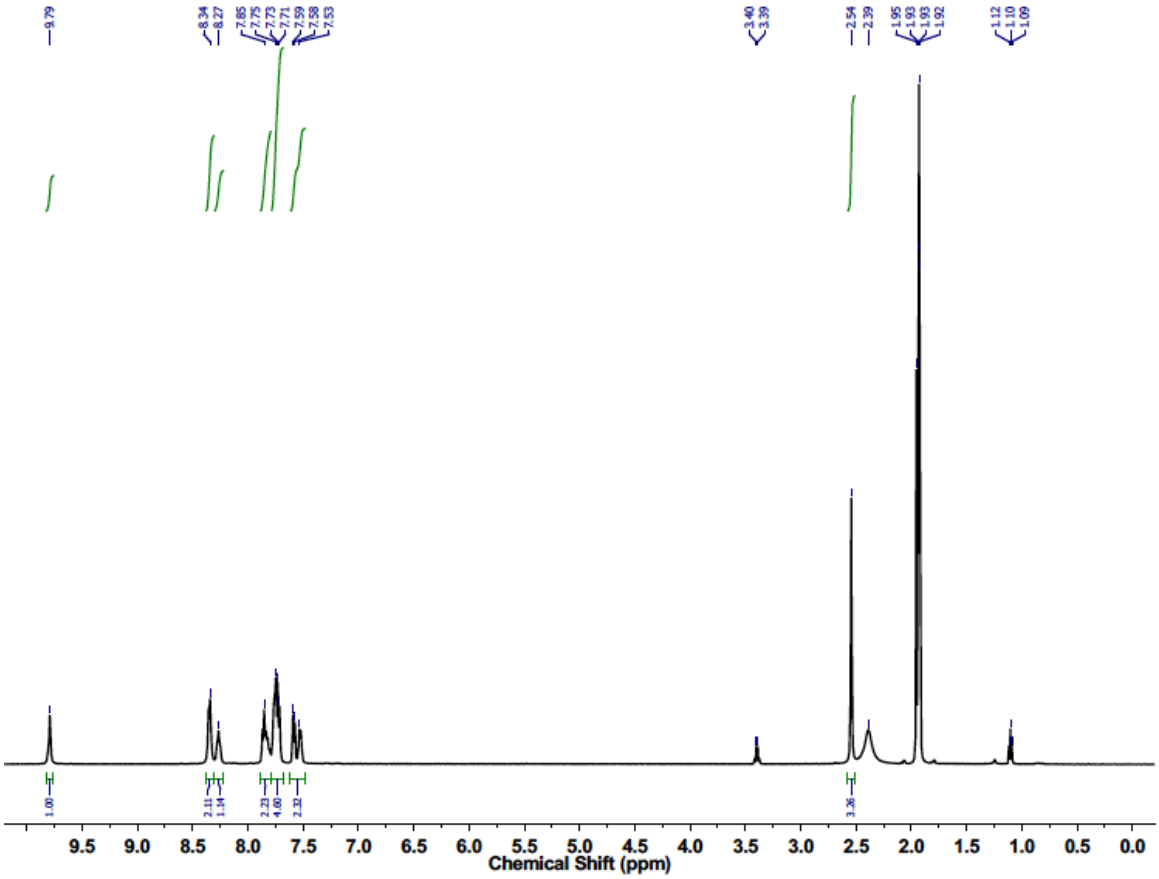

Figure IV.7. ^{1}H NMR spectrum (500 MHz) of $[(_{PhCl}NNS)Fe(CO)_2Br][Fe(CO)_3(Br)_3]$ obtained in CD_3CN at 5 °C.

IR Spectra of NNS Ligands

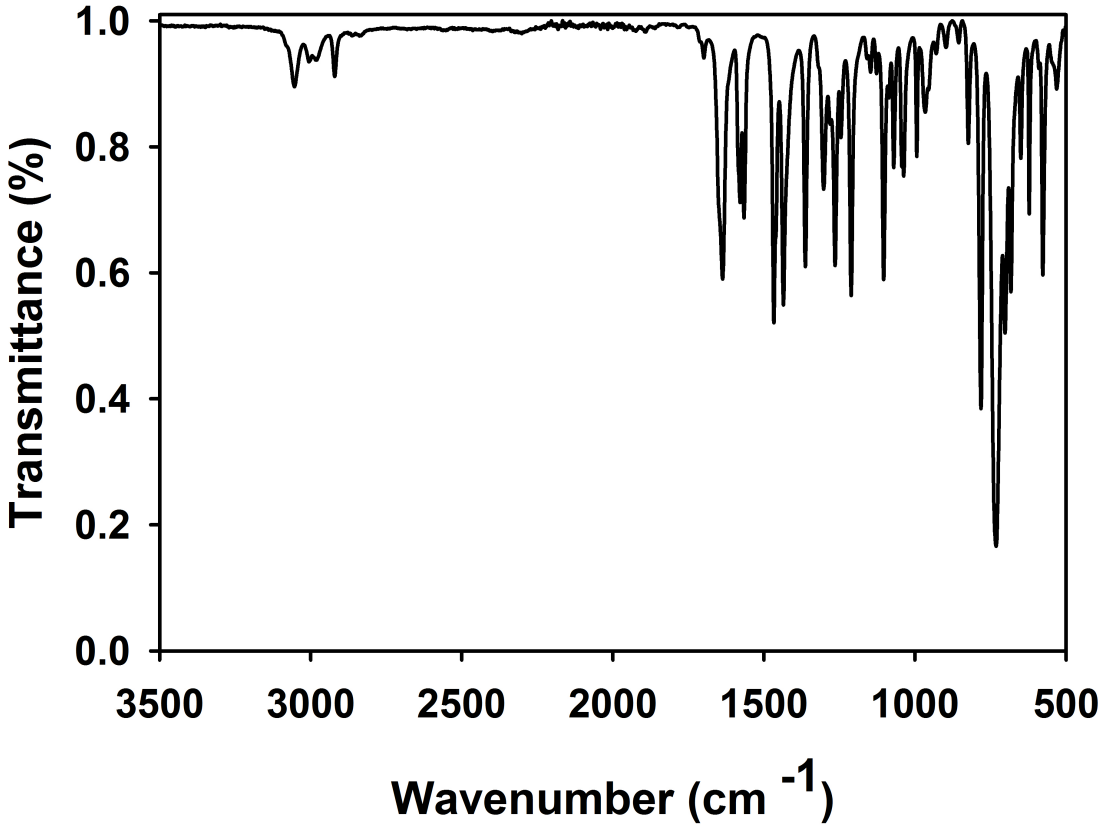

Figure IV.8. Solid state IR spectrum of $N_{Me}NNS$ (298 K, ATR crystal).

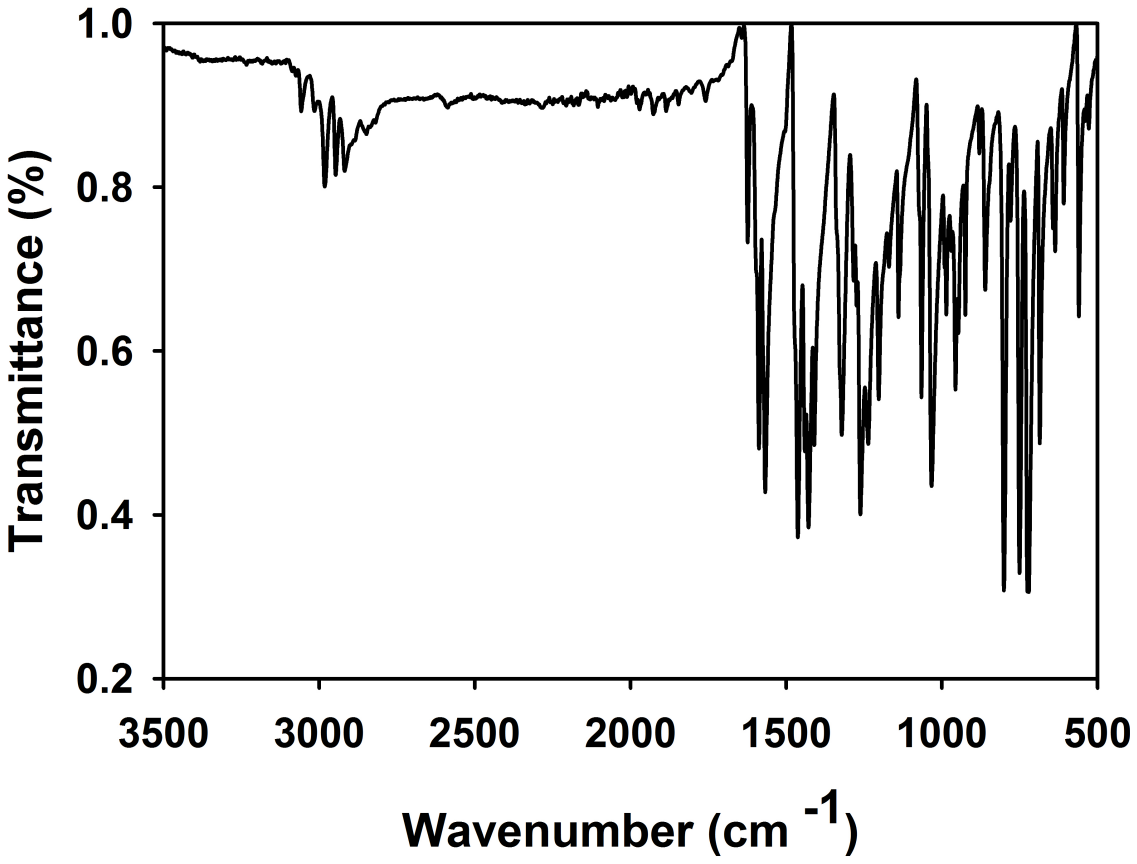

Figure IV.9. Solid state IR spectrum of $_{MeO}$NNNS (298 K, ATR crystal).

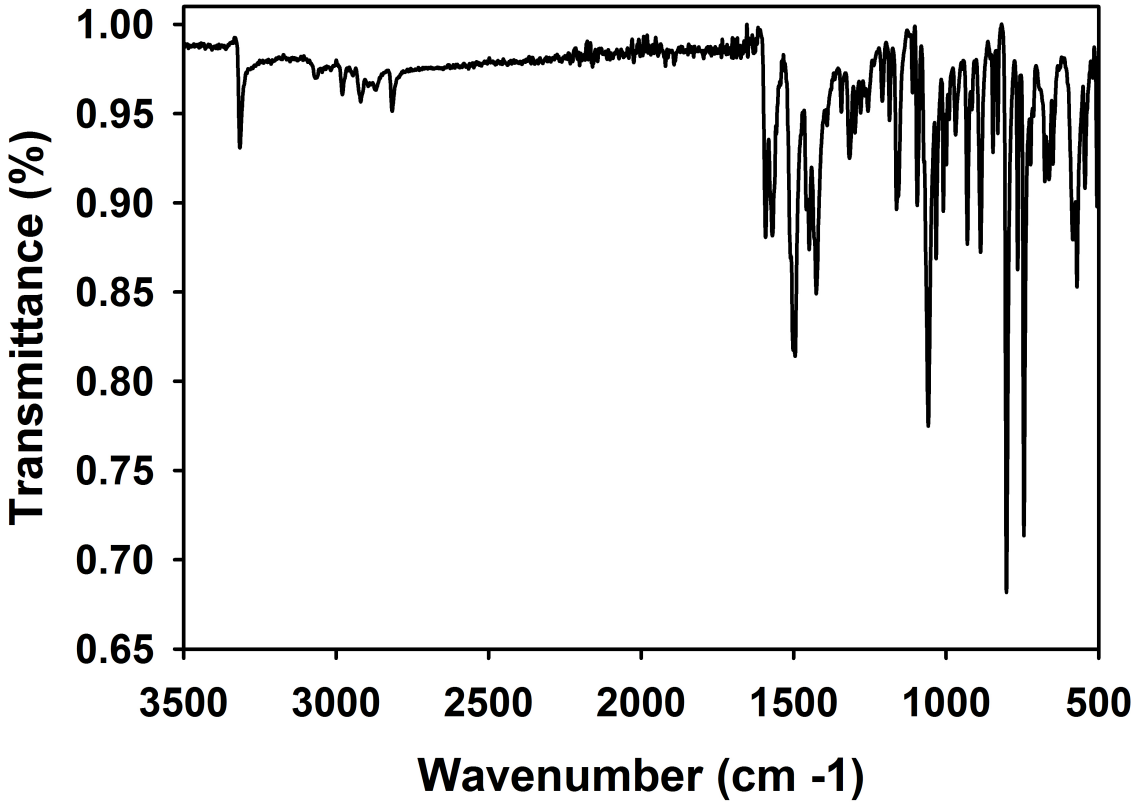

Figure IV.10. Solid state IR spectrum of $_{PhCl}$NNNS (298 K, ATR crystal).

IR Spectra of Iron Complexes

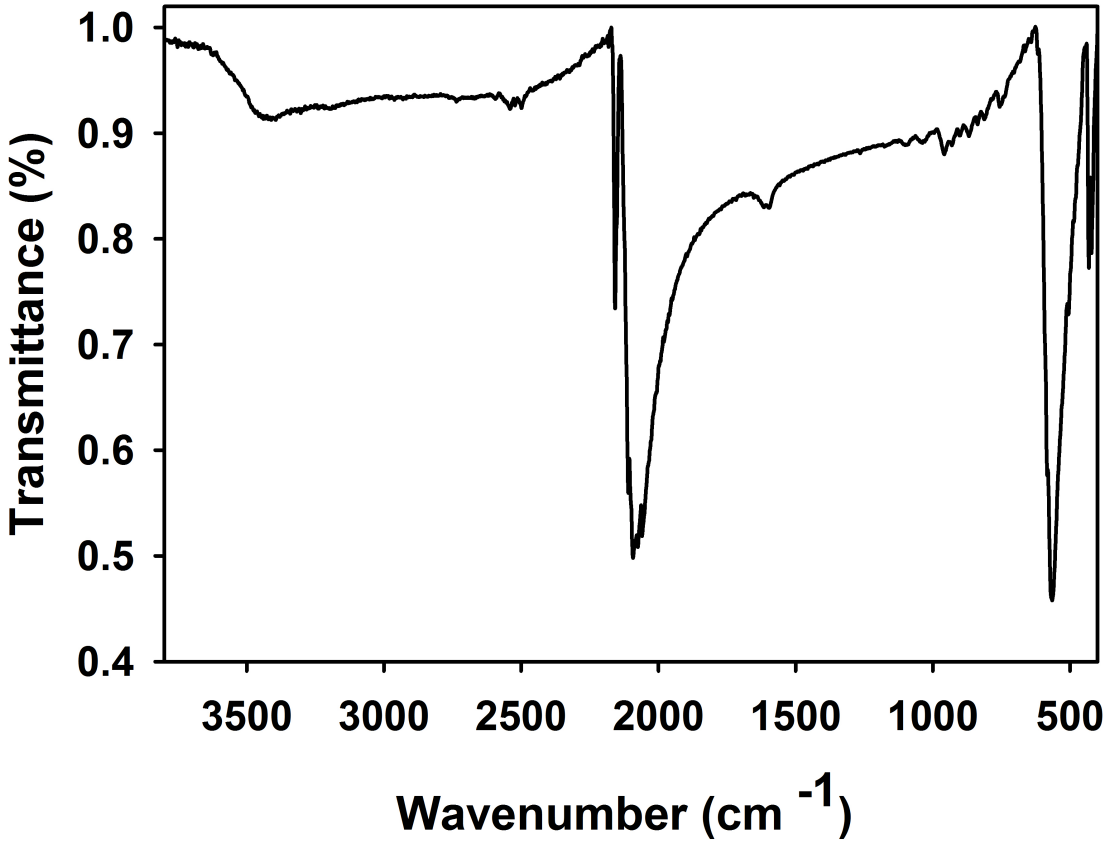

Figure IV.11. Solid state IR spectrum of $[Fe(CO)_4(Br)_2]$ (298 K, ATR crystal).

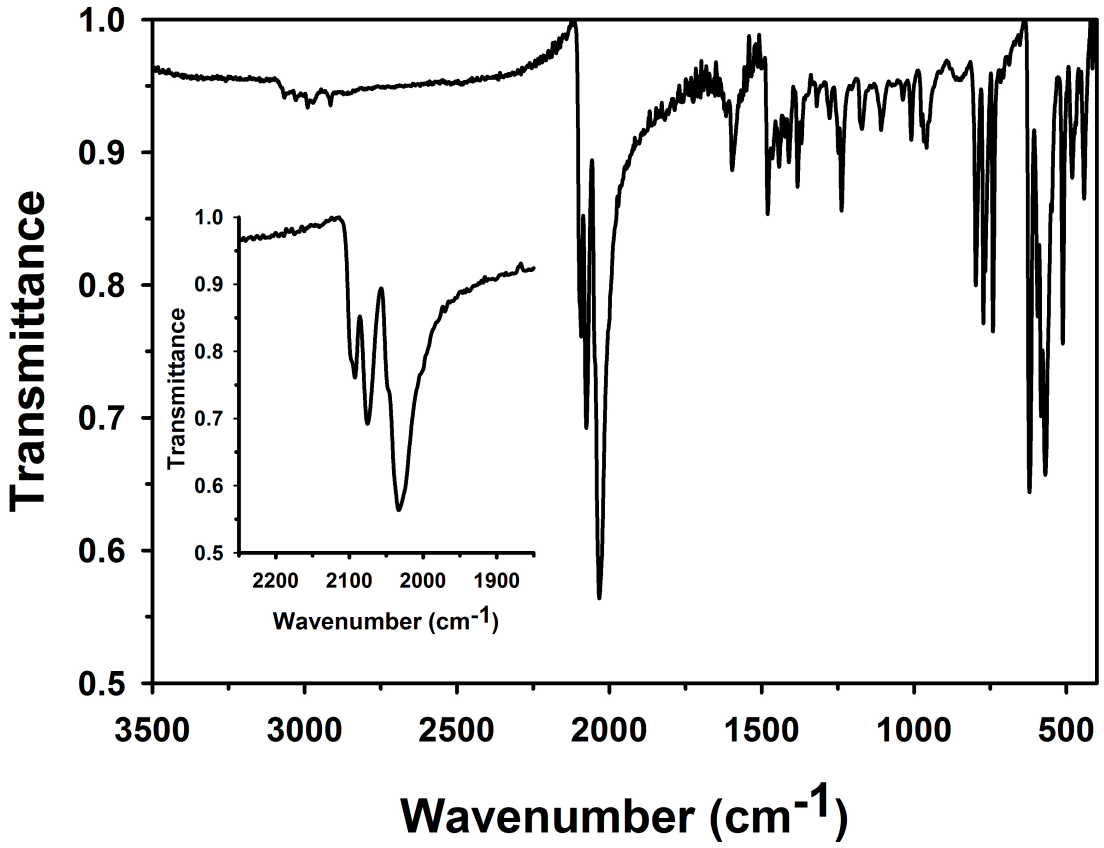

Figure IV.12. Solid state IR spectrum of $[(_{Me}NNS)Fe(CO)_3(Br)][Fe(CO)_3(Br)_3]$ (298 K, ATR crystal).

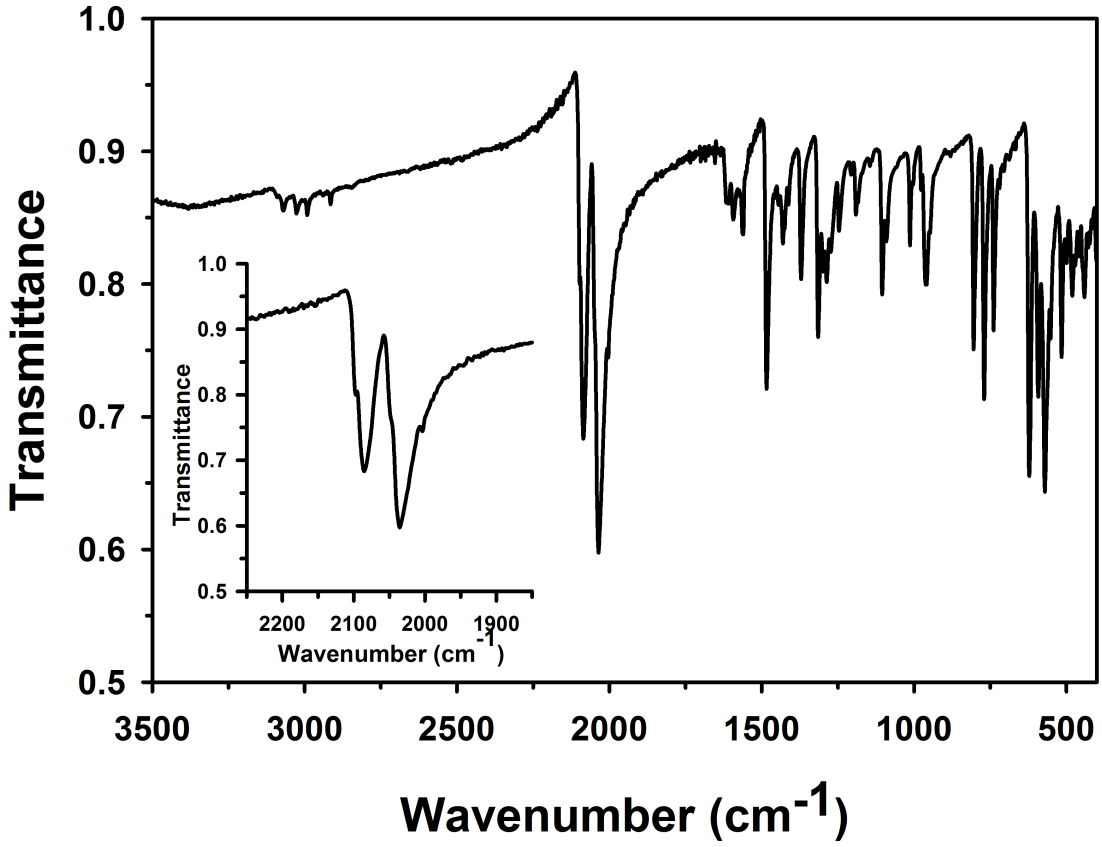

Figure IV.13. Solid state IR spectrum of $[(_{MeO}NNS)Fe(CO)_3(Br)][Fe(CO)_3(Br)_3]$ (298 K, ATR crystal).

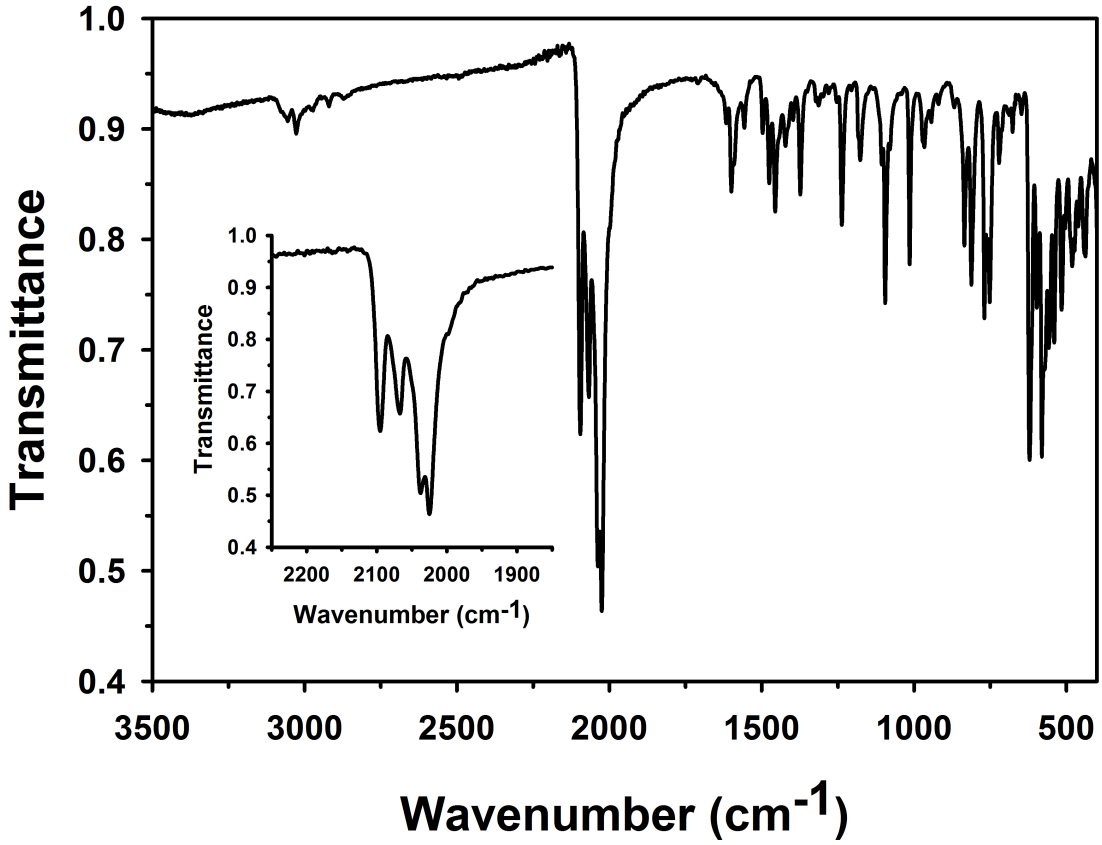

Figure IV.14. Solid state IR spectrum of $[(_{PhCl}NNS)Fe(CO)_3(Br)][Fe(CO)_3(Br)_3]$ (298 K, ATR crystal).

Kinetic Trace for the Iron Carbonyl Complexes.

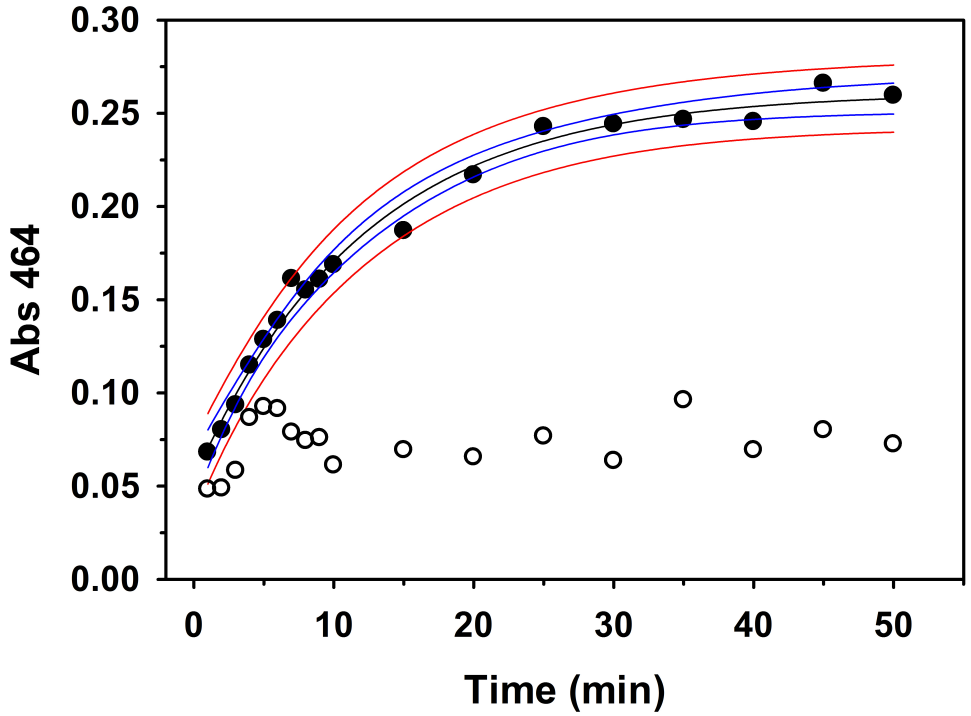

Figure IV.15. $[(_{Me}NNS)Fe(CO)_3(Br)][Fe(CO)_3(Br)_3]$, kinetic trace following the absorbance at $\lambda = 460$ nm as indicator of formation of the dibromide species. Blue lines represent the 95% confidence interval of the exponential fit to the data, and the red lines represent the 95% prediction band. (Shaded circles – time intervals in the presence of light. Un-shaded circles – time intervals in the absence of light).

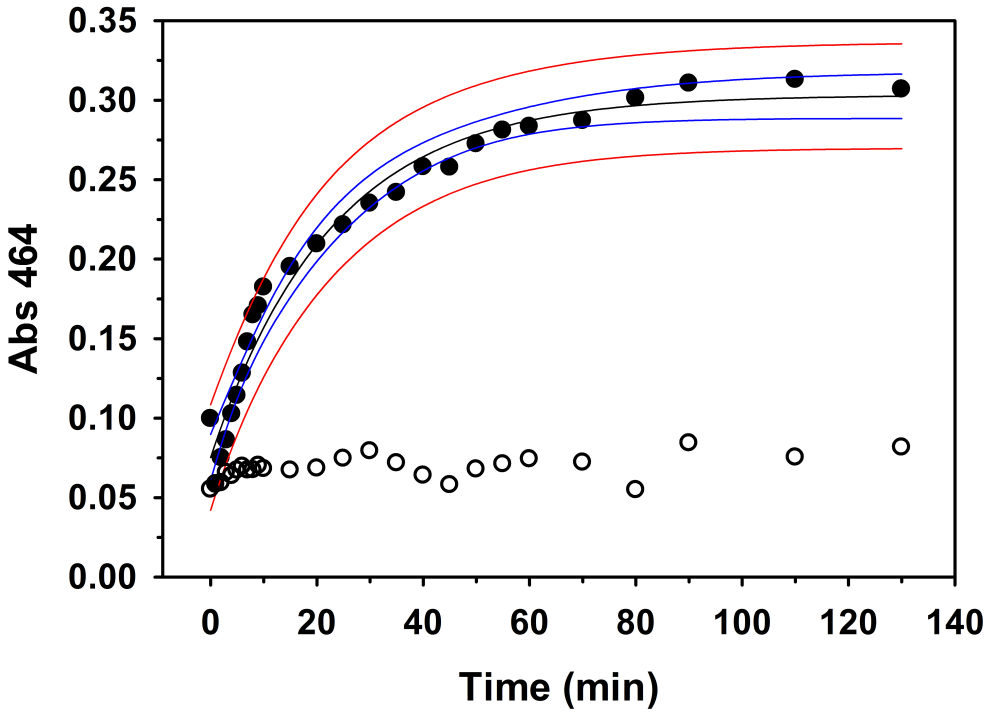

Figure IV.16. [($_{MeO}$NNS)Fe(CO)$_3$(Br)][Fe(CO)$_3$(Br)$_3$], kinetic trace following the absorbance at λ = 460 nm as indicator of formation of the dibromide species. Blue lines represent the 95% confidence interval of the exponential fit to the data, and the red lines represent the 95% prediction band. (Shaded circles – time intervals in the presence of light. Un-shaded circles – time intervals in the absence of light).

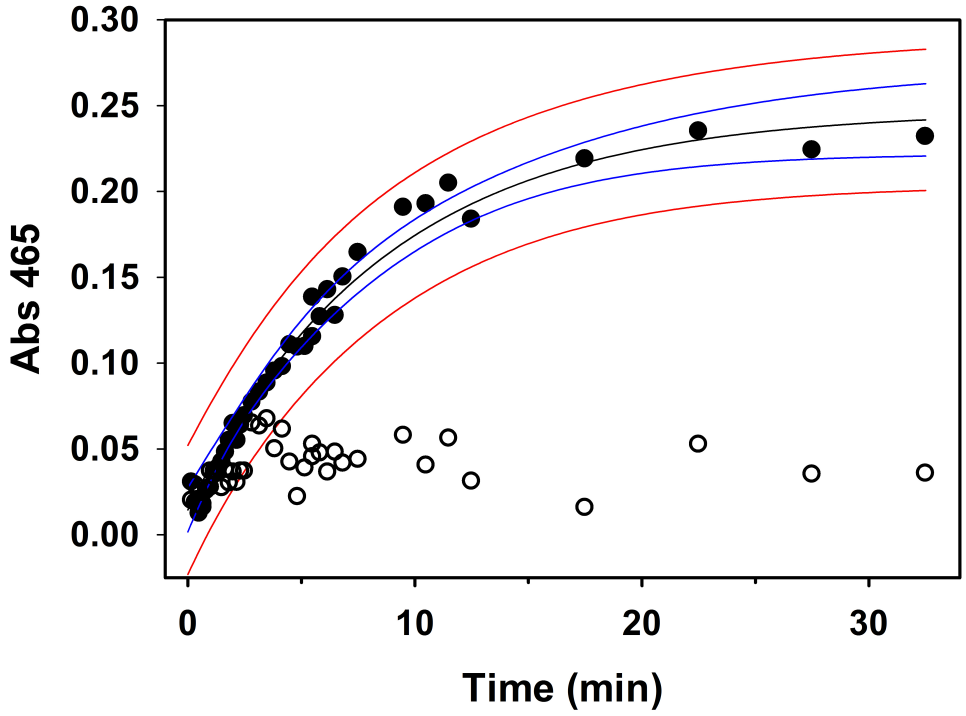

Figure IV.17. [($_{PhCl}$NNS)Fe(CO)$_3$(Br)][Fe(CO)$_3$(Br)$_3$], Kinetic trace following the absorbance at λ = 460 nm as indicator of formation of the dibromide species. Blue lines represent the 95% confidence interval of the exponential fit to the data, and the red lines represent the 95% prediction band. (Shaded circles – time intervals in the presence of light. Un-shaded circles – time intervals in the absence of light).

Summary

1) Metalation reactions involving neutral NNS ligands and Fe(II) tetracarbonyl dibromide starting salt using two different reaction conditions resulted in the formation of the desired complex with their characteristic counter ion.

2) The identity of the counterion varies depending on the reaction conditions and the substituents at the sixth position of the pyridine ring of the NNS ligand. For the low temperature DCM/MeCN reactions less bulkier substituents R= Me, MeO the counter ion X = Br while for R = Q, PhCl, X = $[Fe(CO)_3\ Br_3]$.

3) The dicarbonyl complexes are light sensitive and the varying photostabilities are due to the substituents, concentration and solvent conditions.

4) The iron dicarbonyls exhibit some structural similarity to the apo-active site of mono-iron hydrogenase, and may provide a useful template for future studies into the biogenesis of the unique iron-acyl unit found in the native enzyme.

5. Preliminary studies attempting acyl unit formation on $[(_{Me}NNS)Fe(CO)Br]^+$ with more mild bases (*t*-BuOK, bulky phenoxides, $Ph_3P{=}CH_2$ and CH_3COO^-) did not yield any conversion to the acyl species. Either no reaction or decarbonylation at the metal center was observed.

References

(1) Shima, S.; Pilak, O.; Vogt, S.; Schick, M.; Stagni, M. S.; Meyer-Klaucke, W.; Warkentin, E.; Thauer, R. K.; Ermler. U. *Science* **2008,** *321*, 25.

(2) Wang, X.; Li, Z.; Zeng, X.; Luo, Q.; Evans, D. J.; Pickett, C. J.; Liu, X. *Chem. Commun*. **2008**, 3555.

(3) Hiromoto, T.; Ataka, K.; Pilak, O.; Vogt, S.; Stagni, M. S.; Meyer-Klaucke, W.; Warkentin, E.; Thauer, R. K.; Shima, S.; Ermler. U. *FEBS Lett*. **2009**, *583*, 585.

(4) Schick, M.; Xie, X.; Ataka, K.; Kahnt, J.; Linne, U.; Shima, S. *J. Am. Chem. Soc*. **2012**, *134*, 3271.

(5) Turrell, P. J.; Hill, A. D.; Ibrahim, S. K.; Wright, J. A.; Pickett, C. J. *Dalton Trans.* **2013**, *42*, 8140.

(6) Song, L.-C.; Xie, Z.-J.; Wang, M.-M.; Zhao, G.-Y.; Song, H.-B. *Inorg. Chem.* **2012**, *51*, 7466.

(7) Hu, B.; Chen, D.; Hu, X. *Chem. Eur. J.* **2013**, *19*, 6221.

(8) Hu, B.; Chen, D.; Hu, X. *Chem. Eur. J.* **2014**, *20*, 1.

(9) Turrell, P. J.; Wright, J. A.; Peck, J. N. T.; Oganesyan, V. S.; Pickett, C.J. *Angew. Chem. Int. Ed*. **2010**, *49*, 7508.

(10) Chatterjee, S. K.; Roy, S.; Barman, S. K.; Maji, R. C.; Olmstead, M. M.; Patra, A. K. *Inorg. Chem*. **2012**, *51*, 7625.

(11) Roy, S.; Mitra, P.; Patra , A. K. *Inorg. Chim. Acta*. **2011**, *370*, 247.

(12) Lumsden, S. E. A.; Durgaprasad, G.; Thomas Muthiah, K. A.; Rose, M. J.; *Dalton Trans*. **2014**, 10725.